Hyperfine Splitting in Muonic Hydrogen

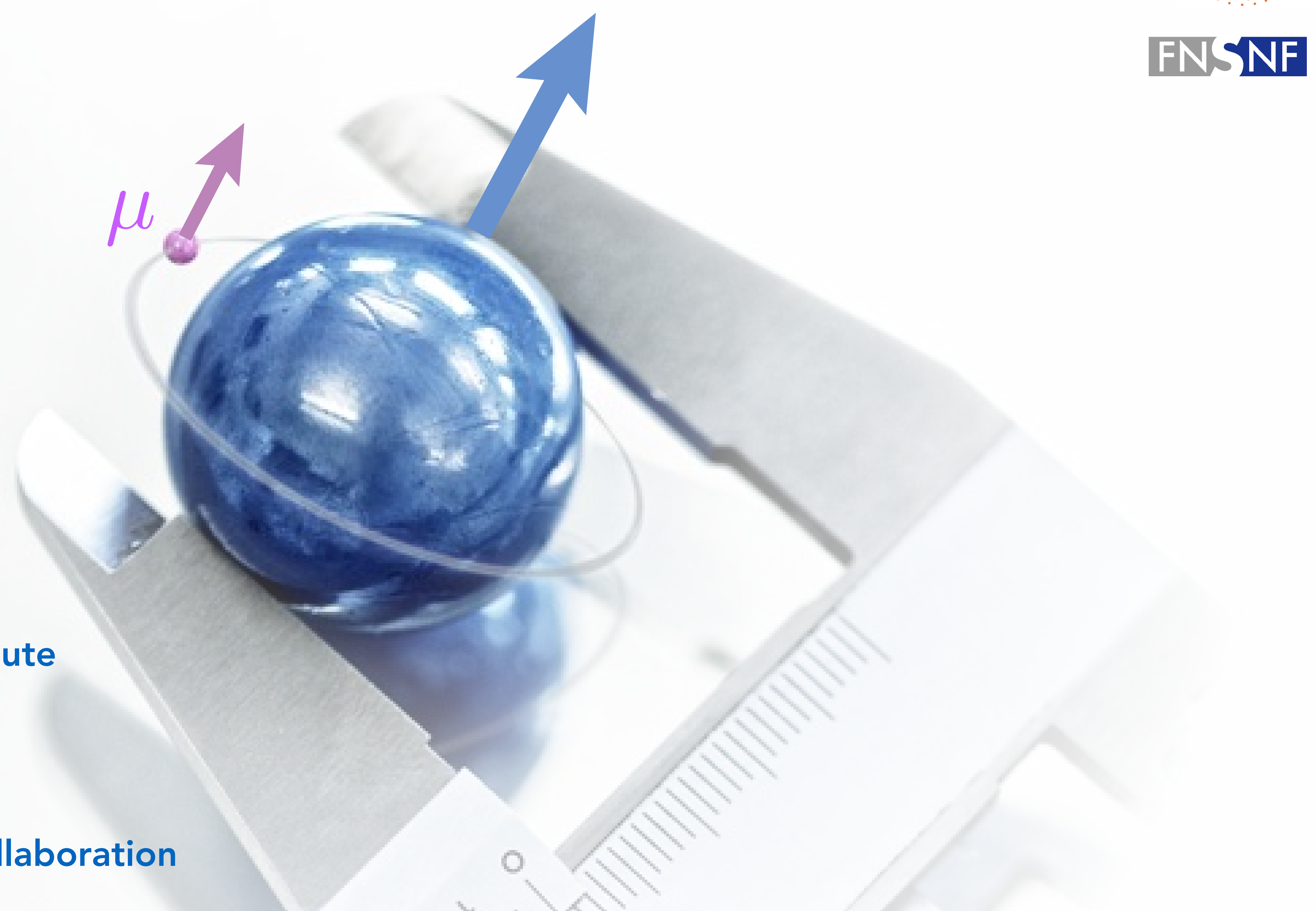

Aldo Antognini

Paul Scherrer Institute
ETH, Zurich
Switzerland

For the CREMA collaboration

Measure 1S-HFS in μp
with 1 ppm accuracy

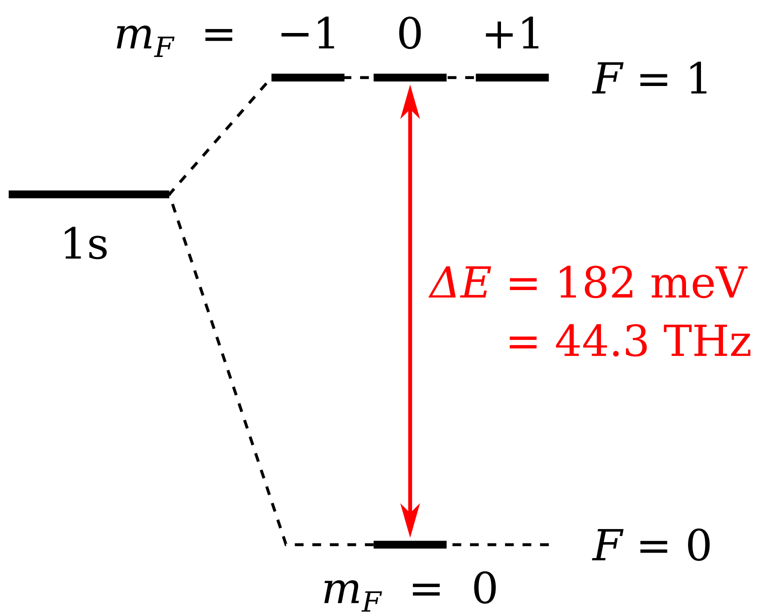

Extract

- 2γ-contribution with $1\text{x}10^{-4}$ rel. accuracy
- Zemach radius r_Z and polarisability Δ_{pol} contribution

$$E_{1S\text{-hfs}} = \Big[\underbrace{182.443}_{E_{\text{F}}}\ \underbrace{+1.350(7)}_{\text{QED+weak}}\ \underbrace{+0.004}_{\text{hVP}}\ \underbrace{-1.30653(17)\left(\frac{r_{Zp}}{\text{fm}}\right) + E_{\text{F}}\left(1.01656(4)\,\Delta_{\text{recoil}} + 1.00402\,\Delta_{\text{pol}}\right)}_{2\gamma\text{ incl. radiative corr.}}\Big]\,\text{meV},$$

AA, Hagelstein, Pascalutsa, arXiv:2205.10076
Peset, Pineda

$$r_Z = -\frac{4}{\pi}\int_0^\infty \frac{\mathrm{d}Q}{Q^2}\left[\frac{G_E(Q^2)G_M(Q^2)}{1+\kappa_N} - 1\right]$$

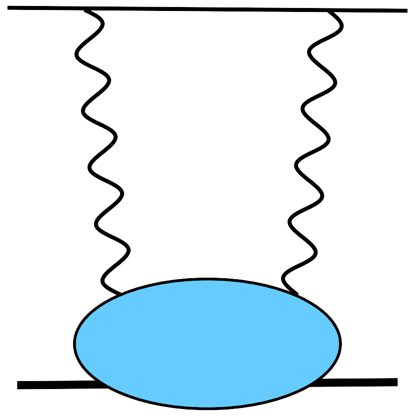

Dispersive approaches

Elastic part (Zemach)

$$\Delta_Z = \frac{8Z\alpha m_r}{\pi}\int_0^\infty \frac{dQ}{Q^2}\left[\frac{G_E(Q^2)G_M(Q^2)}{1+\kappa}-1\right] \equiv -2Z\alpha m_r R_Z,$$

Recoil finite-size

$$\Delta_{\text{recoil}} = \frac{Z\alpha}{\pi(1+\kappa)}\int_0^\infty \frac{dQ}{Q}\left\{\frac{8mM}{v_l+v}\frac{G_M(Q^2)}{Q^2}\left(2F_1(Q^2)+\frac{F_1(Q^2)+3F_2(Q^2)}{(v_l+1)(v+1)}\right) - \frac{8m_r G_M(Q^2)G_E(Q^2)}{Q} - \frac{m}{M}\frac{5+4v_l}{(1+v_l)^2}F_2^2(Q^2)\right\}.$$

Polarisability

$$\Delta_{\text{pol}} = \frac{\alpha m}{2\pi(1+\kappa)M}\left[\Delta_1+\Delta_2\right]$$

$$\Delta_1 = 2\int_0^\infty \frac{dQ}{Q}\left(\frac{5+4v_l}{(v_l+1)^2}\left[4I_1(Q^2)+F_2^2(Q^2)\right] - \frac{32M^4}{Q^4}\int_0^{x_0} dx\, x^2 g_1(x,Q^2) \times\left\{\frac{1}{(v_l+\sqrt{1+x^2\tau^{-1}})(1+\sqrt{1+x^2\tau^{-1}})(1+v_l)}\left[4+\frac{1}{1+\sqrt{1+x^2\tau^{-1}}}+\frac{1}{v_l+1}\right]\right\}\right)$$

$$\Delta_2 = 96M^2\int_0^\infty \frac{dQ}{Q^3}\int_0^{x_0} dx\, g_2(x,Q^2)\left\{\frac{1}{v_l+\sqrt{1+x^2\tau^{-1}}}-\frac{1}{v_l+1}\right\}$$

Alternative approach

$$\Delta_Z = \frac{4\alpha m_r Q_0}{3\pi}\left(-r_E^2 - r_M^2 + \frac{r_E^2 r_M^2}{18}Q_0^2\right) + \frac{8\alpha m_r}{\pi}\int_{Q_0}^{\infty}\frac{dQ}{Q^2}\left(\frac{G_M(Q^2)G_E(Q^2)}{\mu_P}-1\right)$$

Tomalak

Hagelstein, Pascalutsa, Carlson, Martynenko, Tomalak
Faustov, Vanderhaegen, Lensky….

Chiral Perturbation Theory and Dispersive approaches

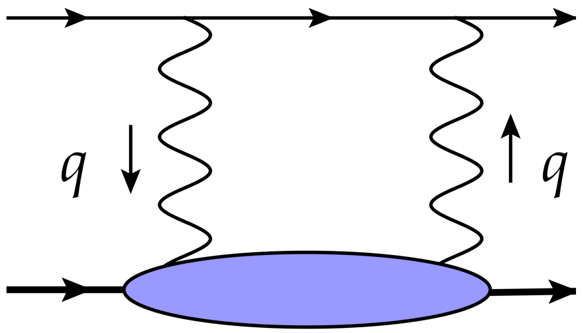

Chiral EFT

Pascalutsa, Hagelstein
Pineda, Peset

Dispersion relation+ data:
$g_1(x,Q^2)$, $g_2(x,Q^2)$, F_1, G_E...

Carlson,
Vanderhaeghen,
Martynenko,
Tomalak,
Pascalutsa,
Hagelstein,

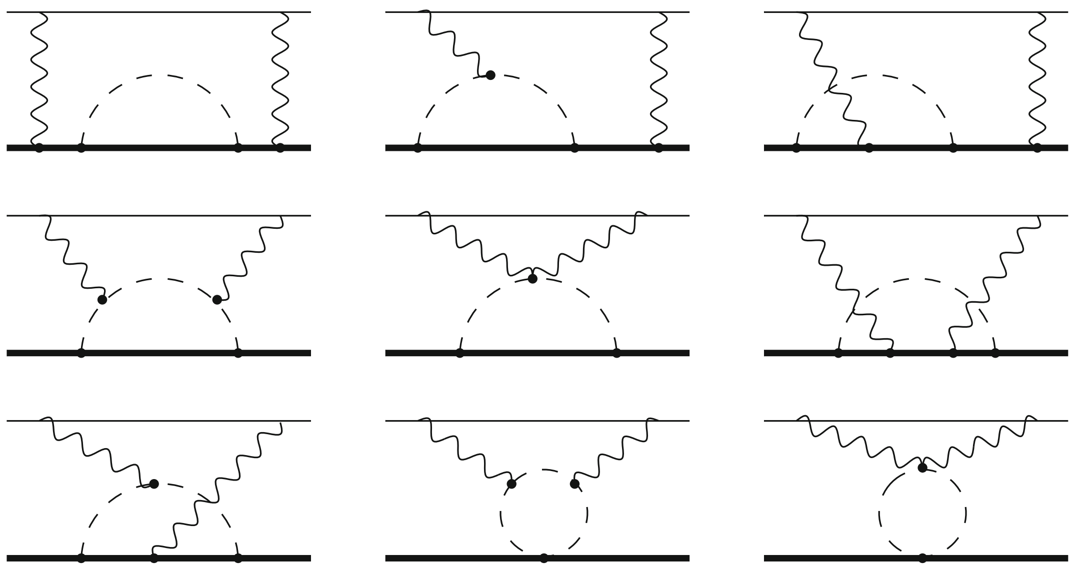

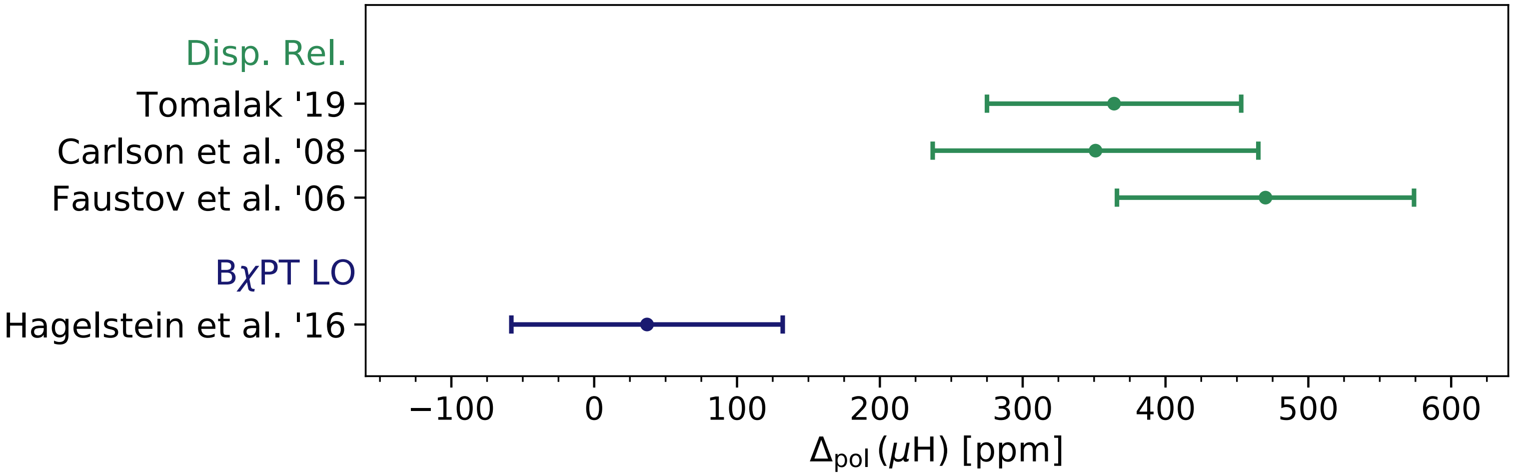

2γ-contribution for the 1S-HFS and Zemach radius

Using Lin, Hammer, Meissner result

$$r_Z = 1.054^{+3}_{-2}\ \text{fm}$$

$$\Delta_Z = -\,7403^{+21}_{-16}\ \text{ppm}$$

Reference	Δ_Z [ppm]	Δ_{recoil} [ppm]	Δ_{pol} [ppm]	Δ_1 [ppm]	Δ_2 [ppm]	$E^{\langle 2\gamma\rangle}_{1S\text{-hfs}}$ [meV]
DATA-DRIVEN						
Pachucki '96 (50)	−8025	1666	0(658)			−1.160
Faustov et al. '01 (138)[a]	−7180		410(80)	468	−58	
Faustov et al. '06 (98)[b]			470(104)	518	−48	
Carlson et al. '11 (99)[c]	−7703	931	351(114)	370(112)	−19(19)	−1.171(39)
Tomalak '18 (139)[d]	−7333(48)	846(6)	364(89)	429(84)	−65(20)	−1.117(19)
HEAVY-BARYON χPT						
Peset et al. '17 (112)						−1.161(20)
LEADING-ORDER χPT						
Hagelstein et al. '16 (62)			37(95)	29(90)	9(29)	
+ Δ(1232) EXCIT.						
Hagelstein et al. '18 (101)			−13	84	−97	

AA, Hagelstein, Pascalutsa, arXiv:2205.10076

Table 2 Determinations of the proton Zemach radius r_{Zp}, in units of fm.

ep scattering		μH 2*S* hfs		H 1*S* hfs	
Lin *et al.* (26)	Borah *et al.* (91)	Antognini *et al.* (2)	BχPT (62)	Volotka *et al.* (92)	BχPT (62)
$1.054^{+0.003}_{-0.002}$	1.0227(107)	1.082(37)	1.041(31)	1.045(16)	1.012(14)

What happened in the last years: shrinking the uncertainty

- First ChPT results of polarisability contribution — Hagelstein & Pascalutsa
- New data from g2p available
- Precision values of the Zemach radius r_Z — $\Delta_Z E_F = -1.3506^{+38}_{-29}$ meV — Lin et al., Borah et al., Distler et al.,
- Scaling the 2γ-contribution from H — $\Delta E^{2\gamma+hVP} = -1.159(2)$ meV — Pineda, Peset; Tomalak; AA, Hagelstein & Pascalutsa

Zemach, polarisability, recoil, eVP correction to 2γ, hVP

AA, Hagelstein, Pascalutsa, arXiv:2205.10076

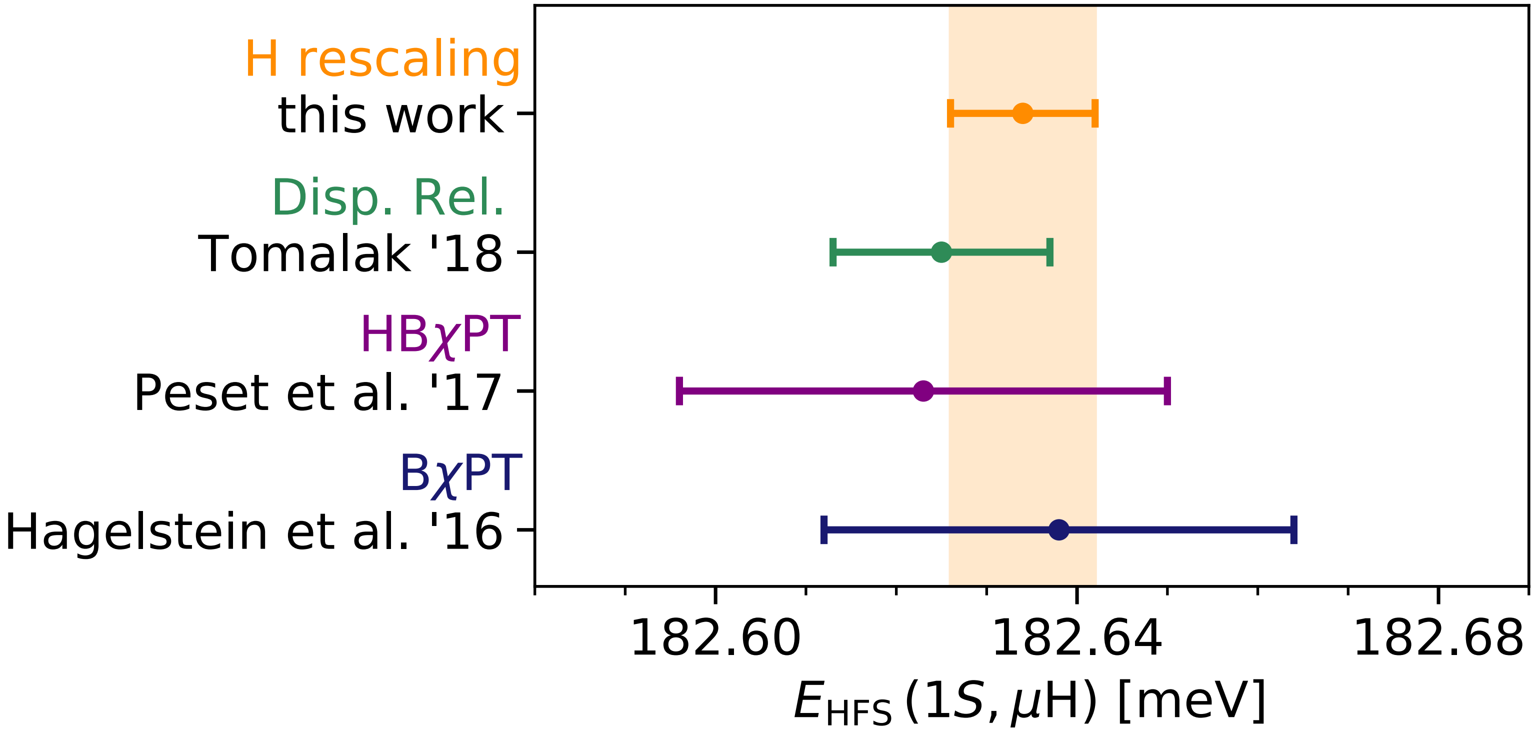

Compared to results without re-scaling from H the uncertainty has decreased by a factor of 5

$\Delta E_{1S-HFS} = 182.634(8)$ meV

limited by QED

2S-2P versus HFS

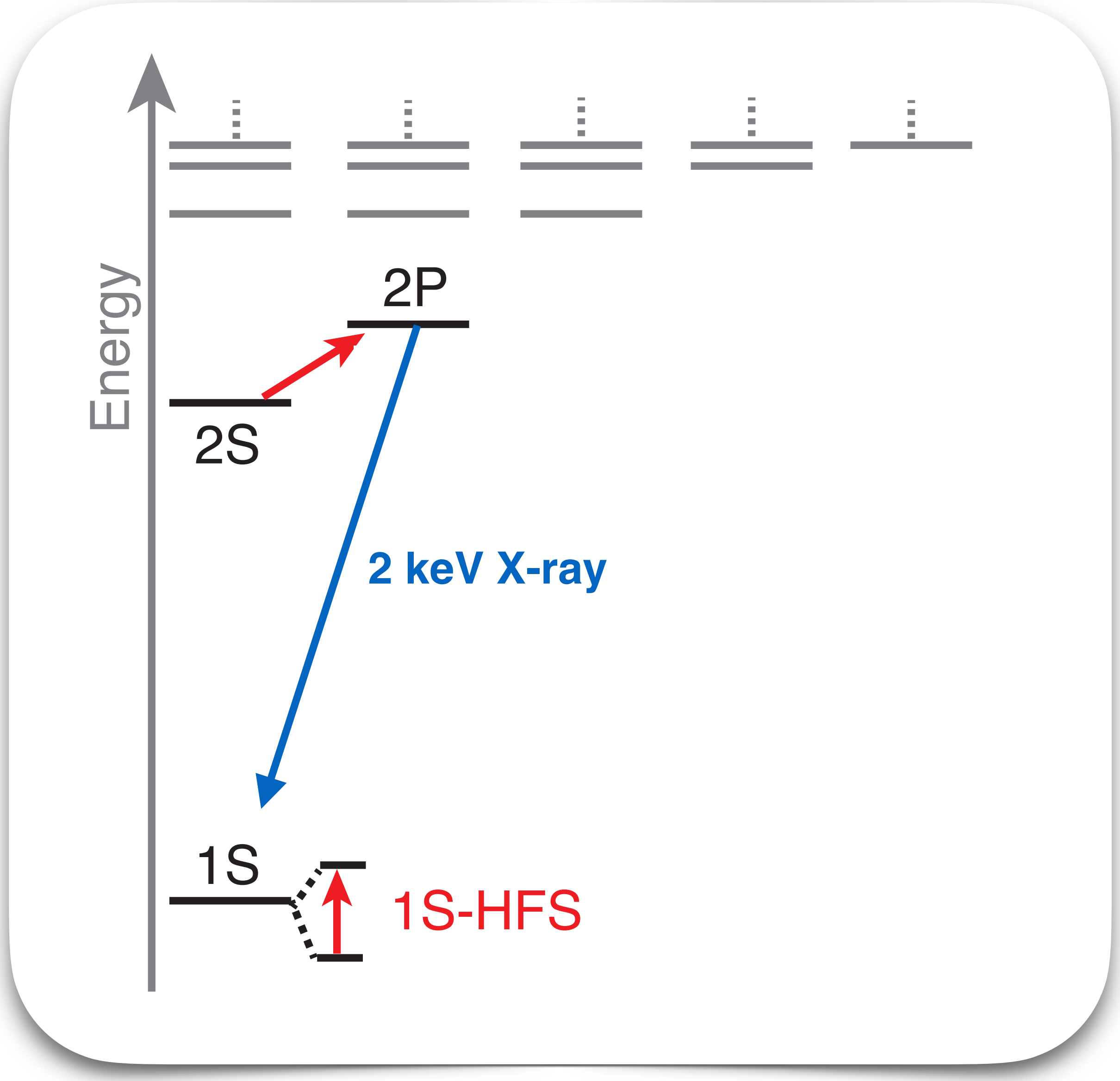

- Excite the 2S-2P transition at 6.0 μm
- Detect the 2 keV X-ray from 2P→1S de-excitation

- Excite the HFS transition at 6.8 μm
- But what do we detect?

The principle

- Stop muon beam in 1 mm H_2 gas target at 22 K, 0.5 bar
- Wait until μp atoms de-excite and thermalize
- Laser pulse: μp(F=0) + γ → μp(F=1)
- De-excitation: μp(F=1) + H_2→μp(F=0) + H_2 + E_{kin}
- μp diffuses to Au-coated target walls
- formed μAu* de-excites producing X-rays
- Plot number of X-ray events vs laser frequency

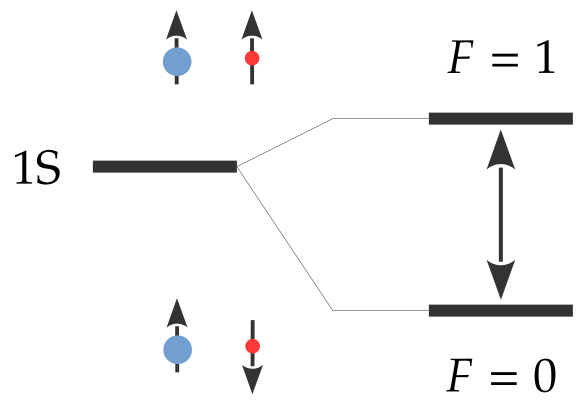

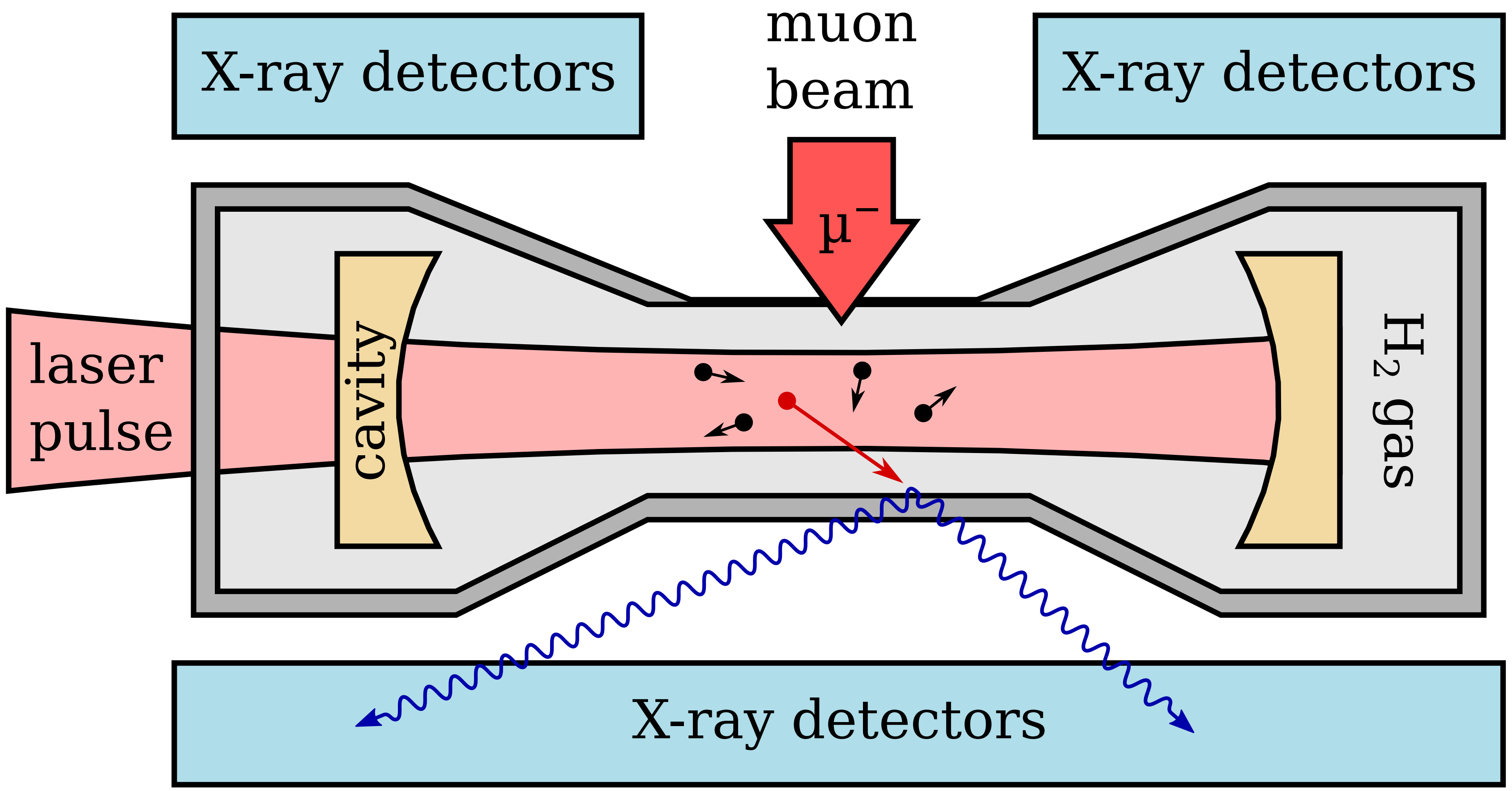

The principle

- Stop muon beam in 1 mm H_2 gas target at 22 K, 0.5 bar
- Wait until μp atoms de-excite and thermalize
- Laser pulse: μp(F=0) + γ → μp(F=1)
- De-excitation: μp(F=1) + H_2 → μp(F=0) + H_2 + E_{kin}
- μp diffuses to Au-coated target walls
- formed μAu* de-excites producing X-rays
- Plot number of X-ray events vs laser frequency

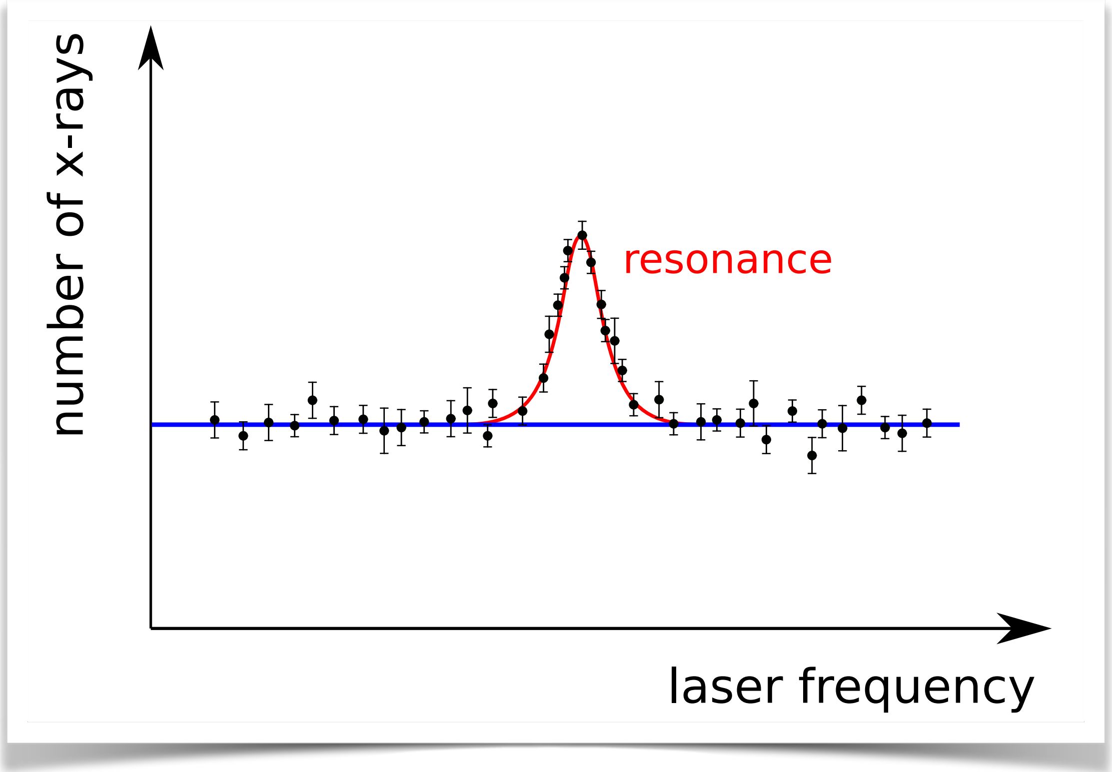

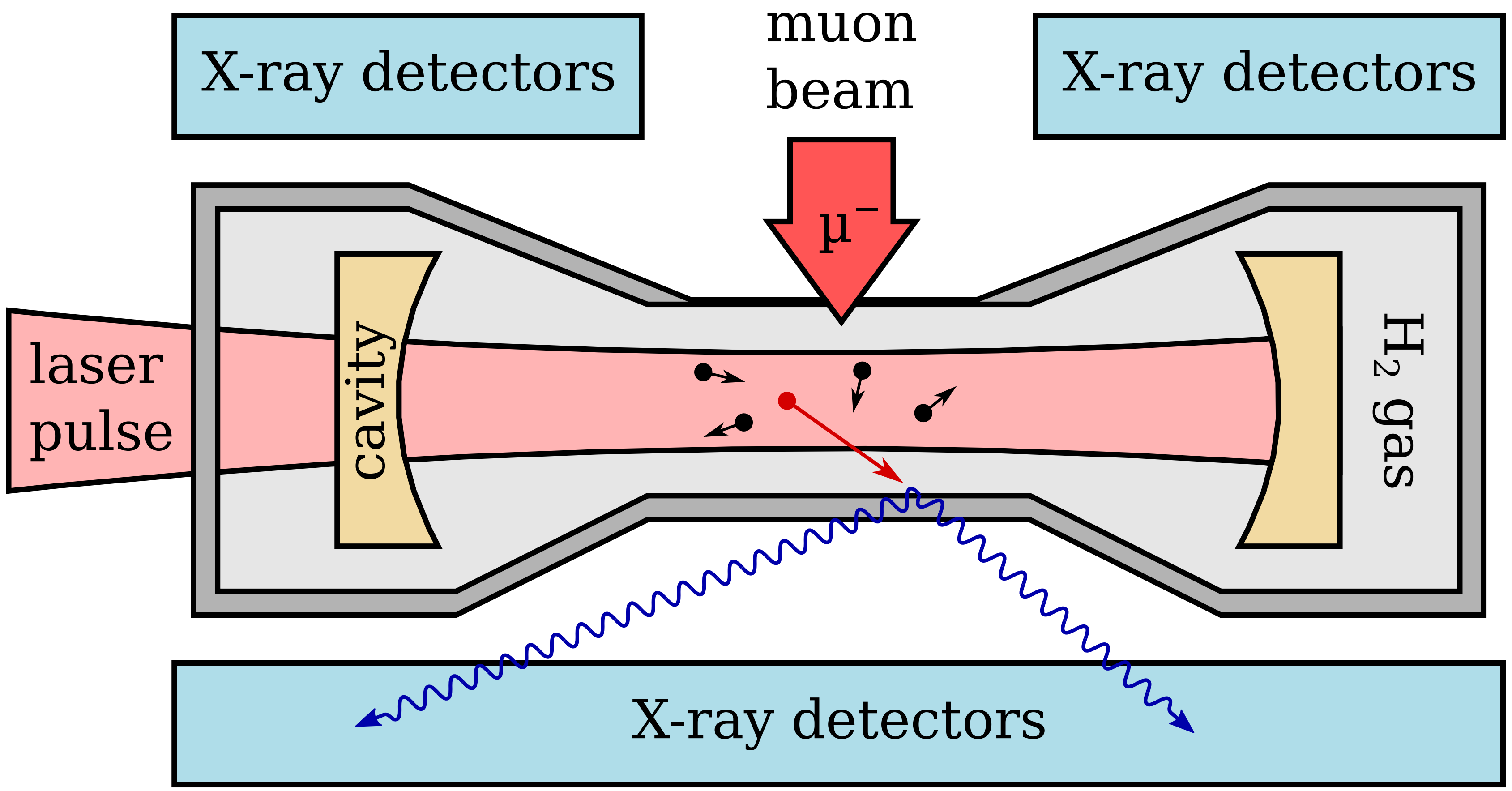

μp formation and thermalisation

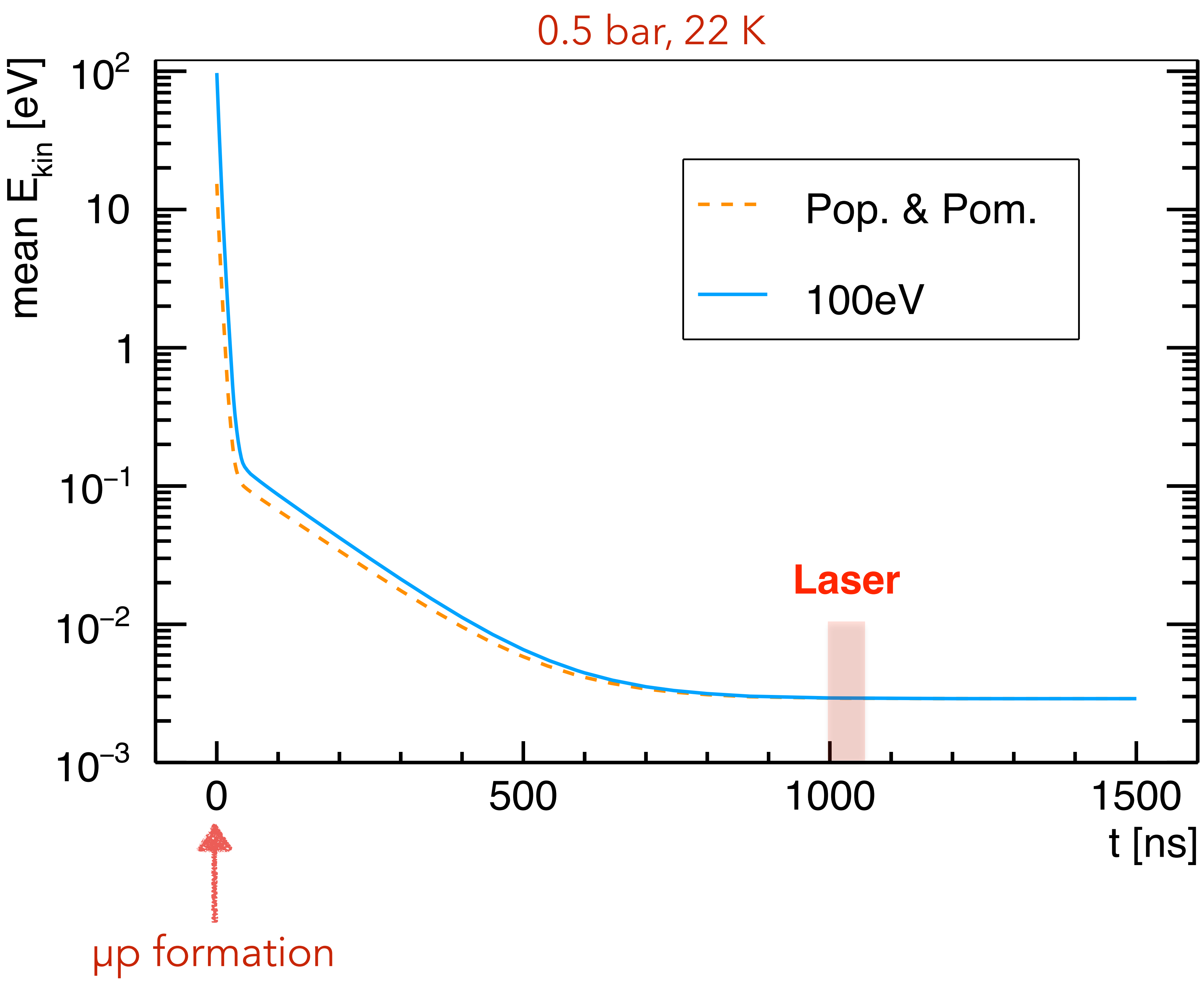

- μp atoms formed in highly excited states
- De-excitation to 1S-state imparts kinetic energies up to 100 eV
- μp has to thermalise before we can excite it with laser light

Laser excitation

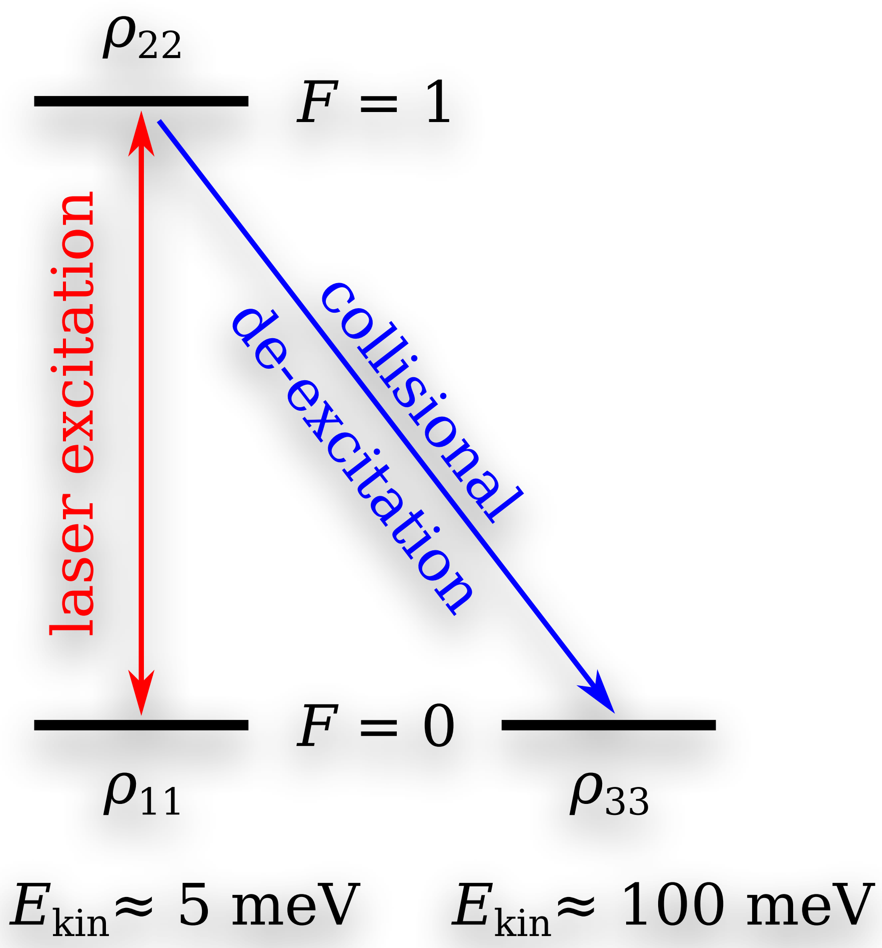

- We modelled the laser excitation using optical Bloch equations including
  - Inelastic collisions: part of the detection scheme
  - Elastic collisions: additional decoherence effect
  - Laser bandwidth
- Included Doppler broadening
- Accounted for ortho-para H_2 ro-vibrational levels

Amaro, et al., arXiv:2112.00138

Transition	$\mathcal{M}$ [m]	$\frac{\Omega}{\sqrt{\mathcal{I}}}$ [m/$\sqrt{\text{Js}}$]
$2s^{F=1} \rightarrow 2p^{F=2}_{3/2}$	$\sqrt{5}a_\mu = 6.367 \times 10^{-13}$	2.65×10^4
$1s^{F=0} \rightarrow 1s^{F=1}$	$\frac{\hbar}{4m_\mu c}\left(g_\mu + \frac{m_\mu}{m_p} g_p\right) = 1.228 \times 10^{-15}$	5.12×10^1

Laser excitation

0.5 bar, 22 K

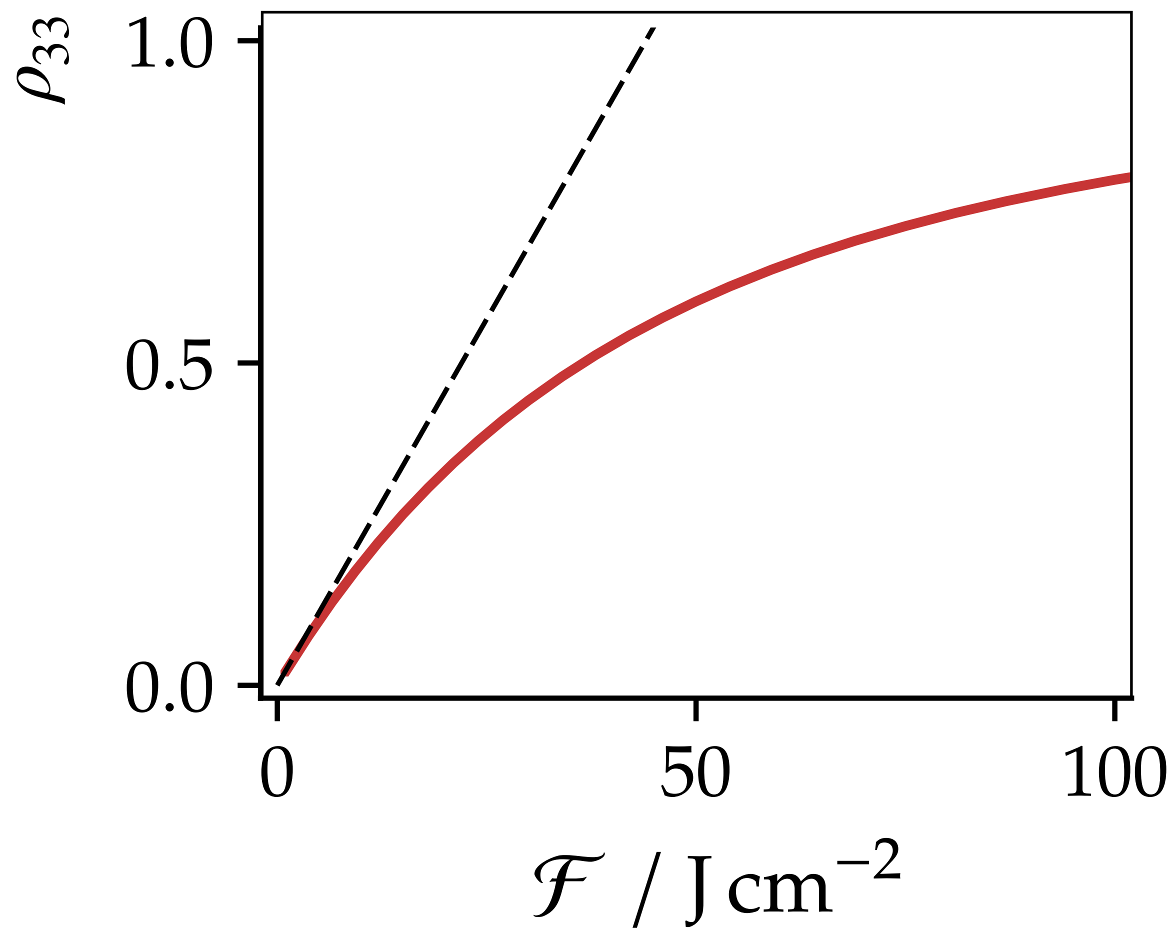

0.5 bar, 22 K

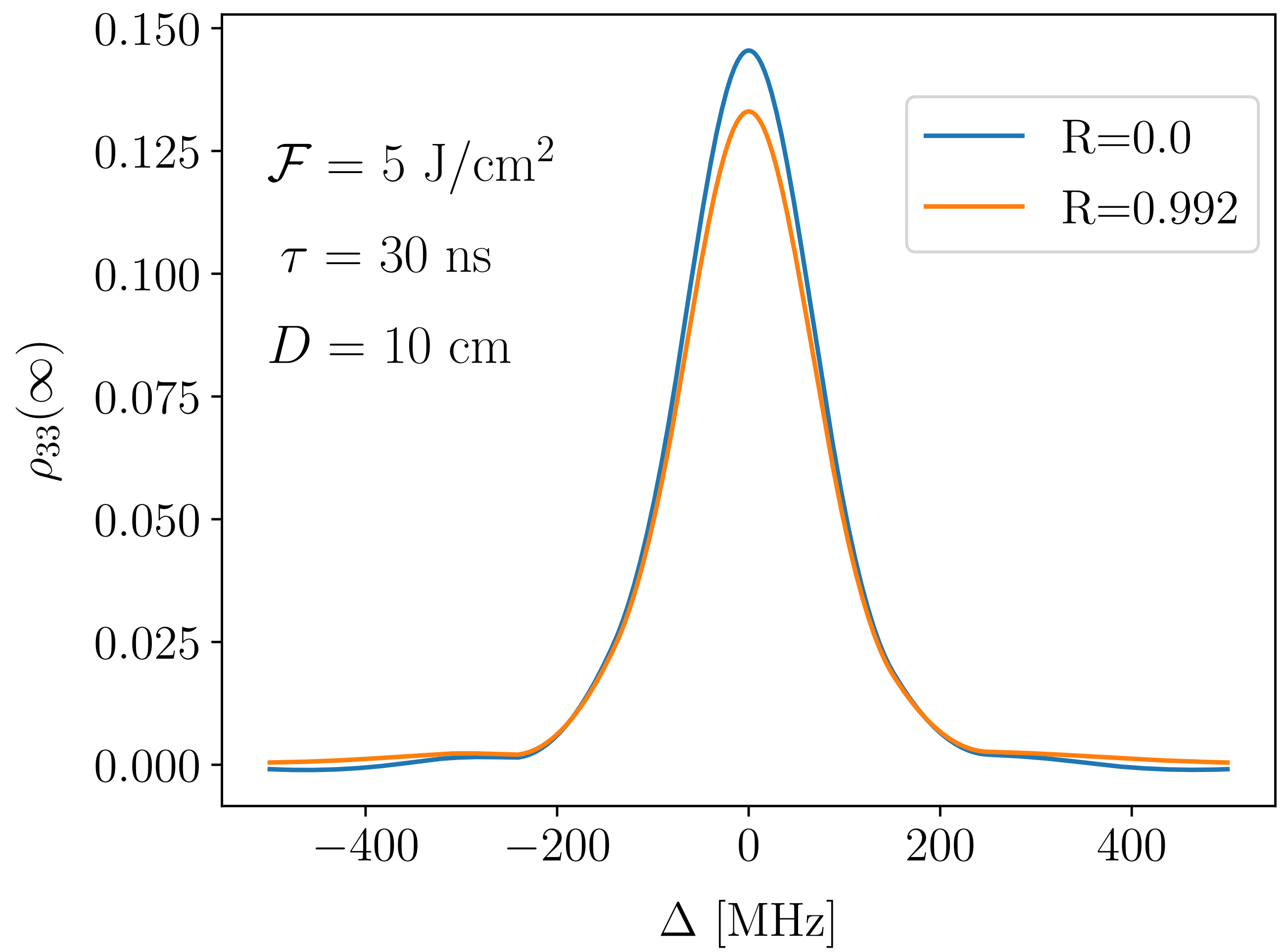

Transition	Linewith	Saturation fluence
2S-2P	20 GHz	0.016 J/cm^2
HFS	200 MHz	44 J/cm^2

Thermalised versus laser excited μp atoms

- De-excitation: μp(F=1) + H_2 → μp(F=0) + H_2 + E_{kin}
- μp diffuses to Au-coated target walls

Kinetic energy distribution with/without laser excitation

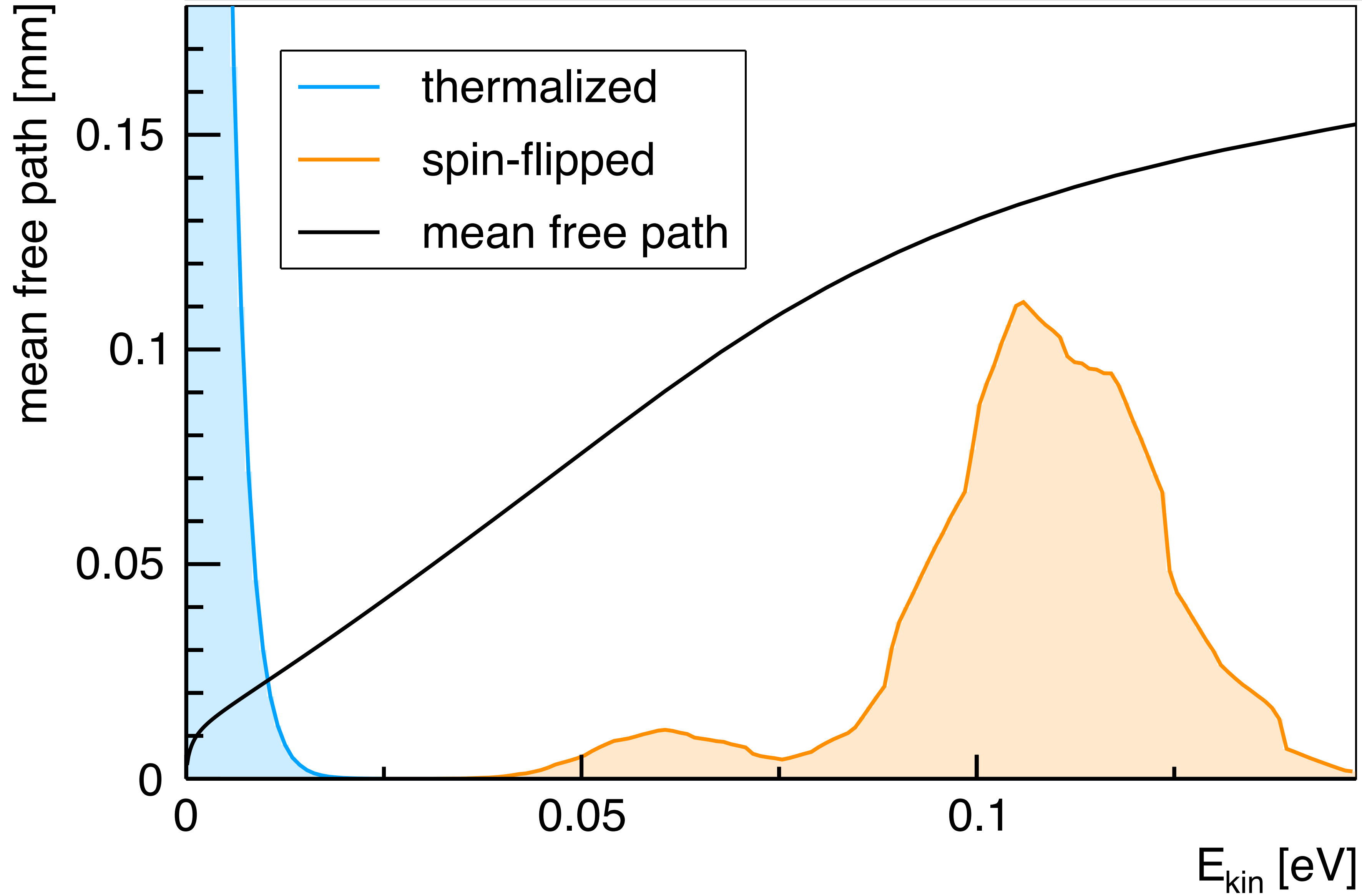

On average μp atoms wins 0.1 eV kinetic energy after a successful laser excitation

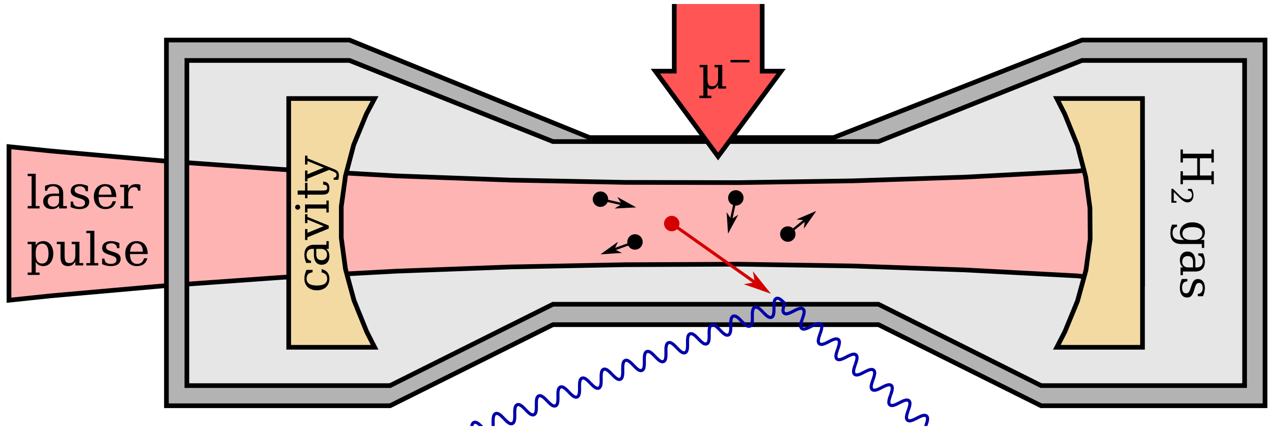

Diffusion to the target walls

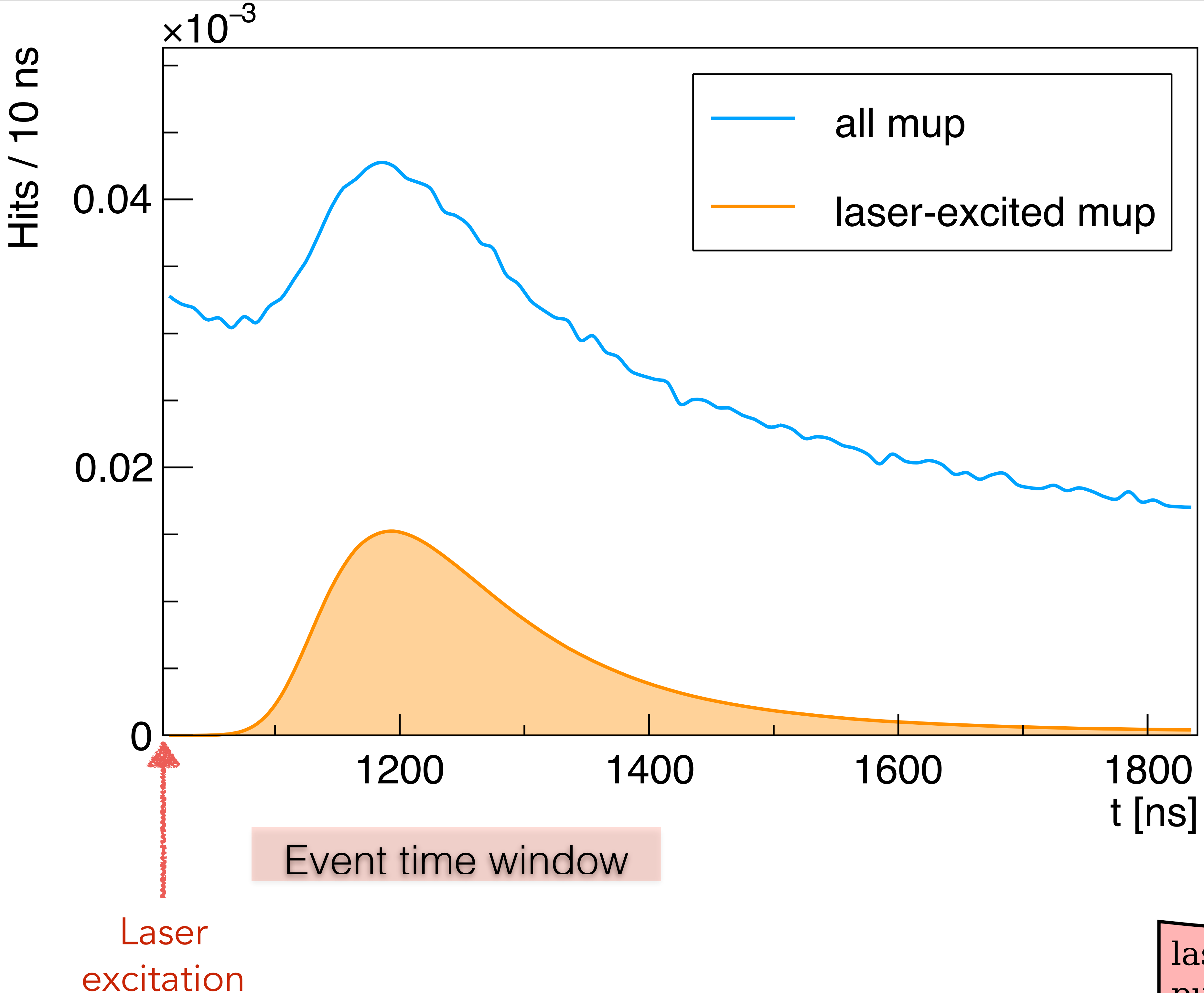

- 100 ns after laser excitation the first μp atoms reach the target walls
- Signal on top of a large background from μp atoms formed closed to the target walls

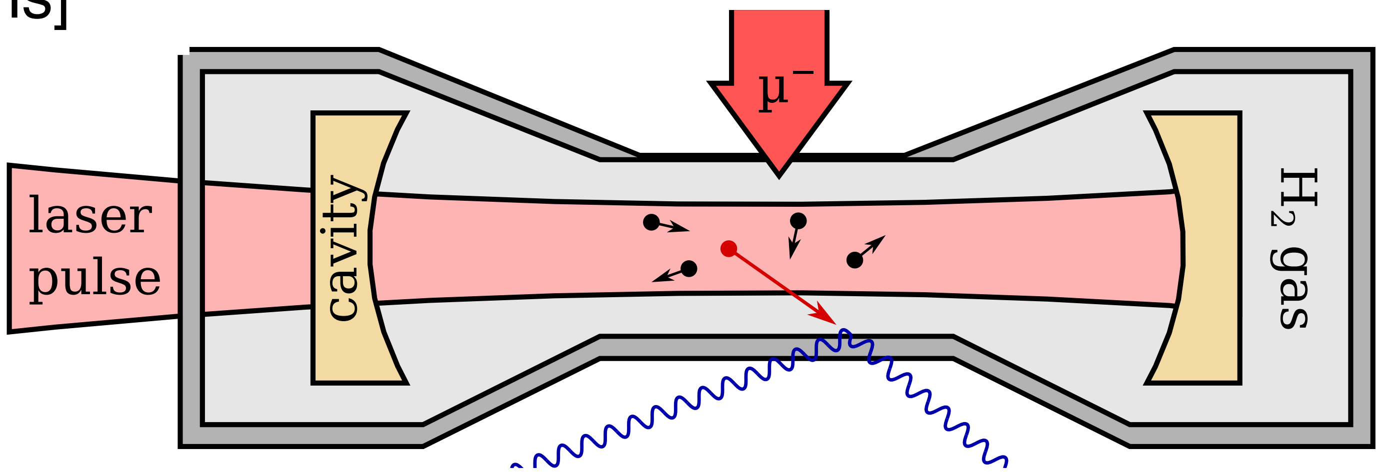

Upon arrival at the target walls

$$\mu\mathrm{p} + \mathrm{Au} \rightarrow \mu\mathrm{Au}^* + \mathrm{p}$$
$$\downarrow$$
$$\mu\mathrm{Au} + \text{X-rays}$$
$$\downarrow$$
$$\nu + \ldots + \text{neutrons} + \gamma + p, d, \alpha$$

(n→n')	Energy	Prob.
2→1	5.6 MeV	90%
3→2	2.4 MeV	84%
4→3	0.9 MeV	76%
.....	.....	.....

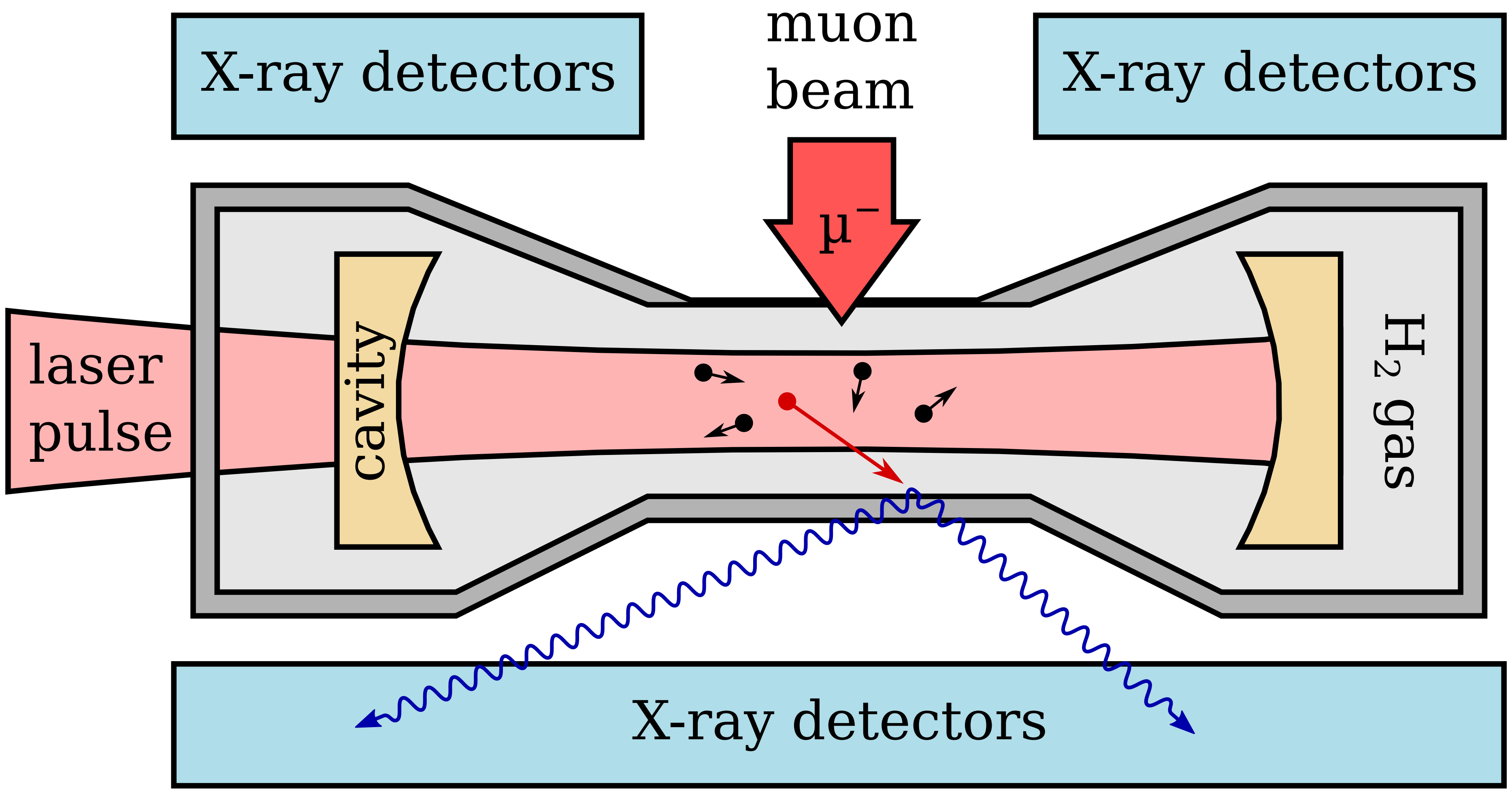

Background sources

Diffusion background

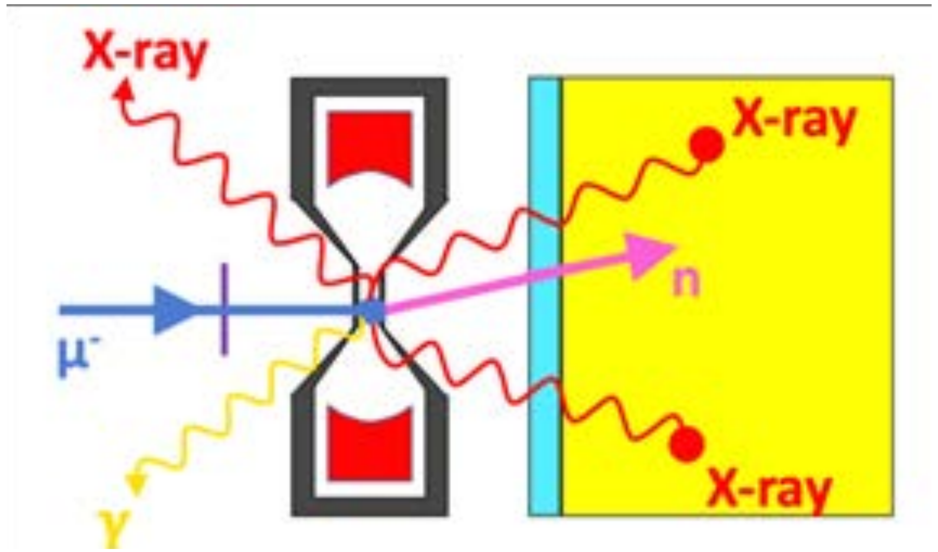

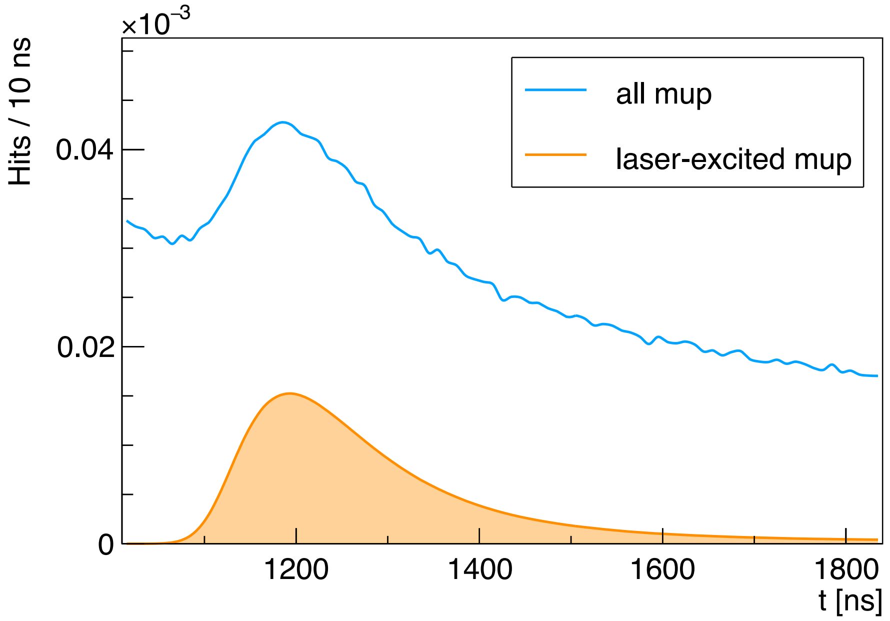

Bremsstrahlung background

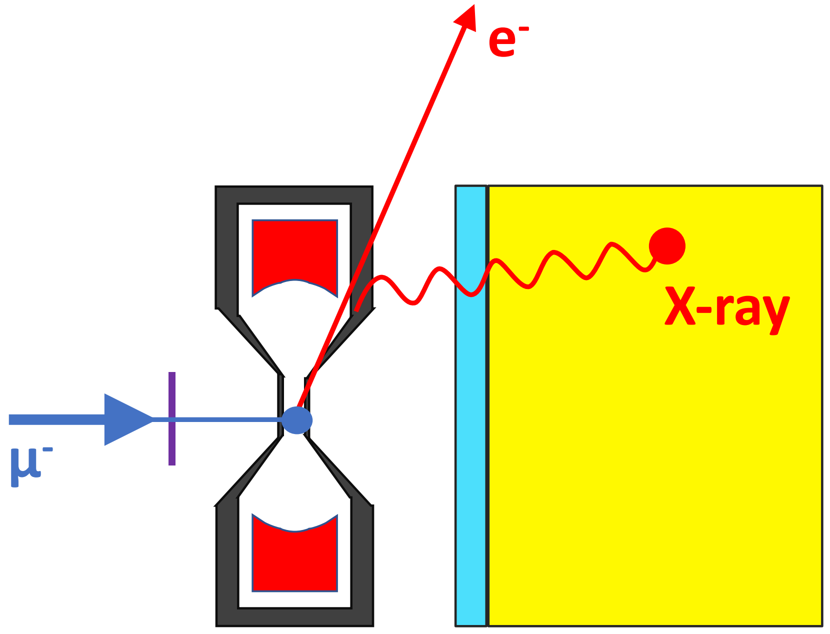

- Muon decay followed by Bremsstrahlung

$$\mu \rightarrow e + \nu + \bar{\nu}$$
$$\downarrow$$
$$\text{Bremstrahlung} + \ldots.$$

Factor of 10 more muon-decays than laser-excited μp reaching the target walls

Uncorrelated background

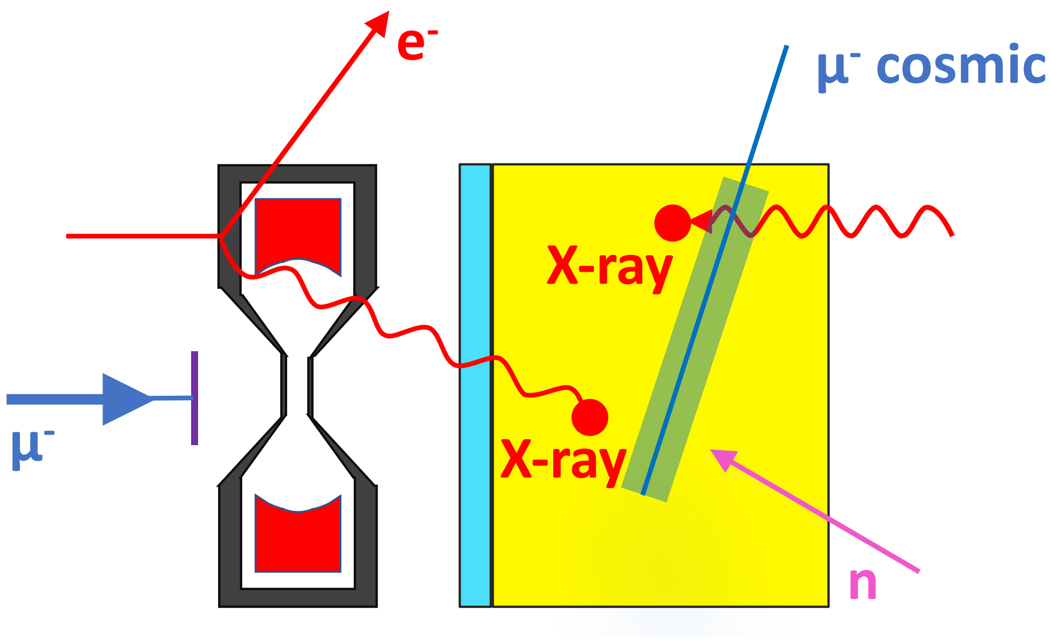

- Beam electrons
- Radioactivity of the beamline
- Neutrons

Detection system prototype tested

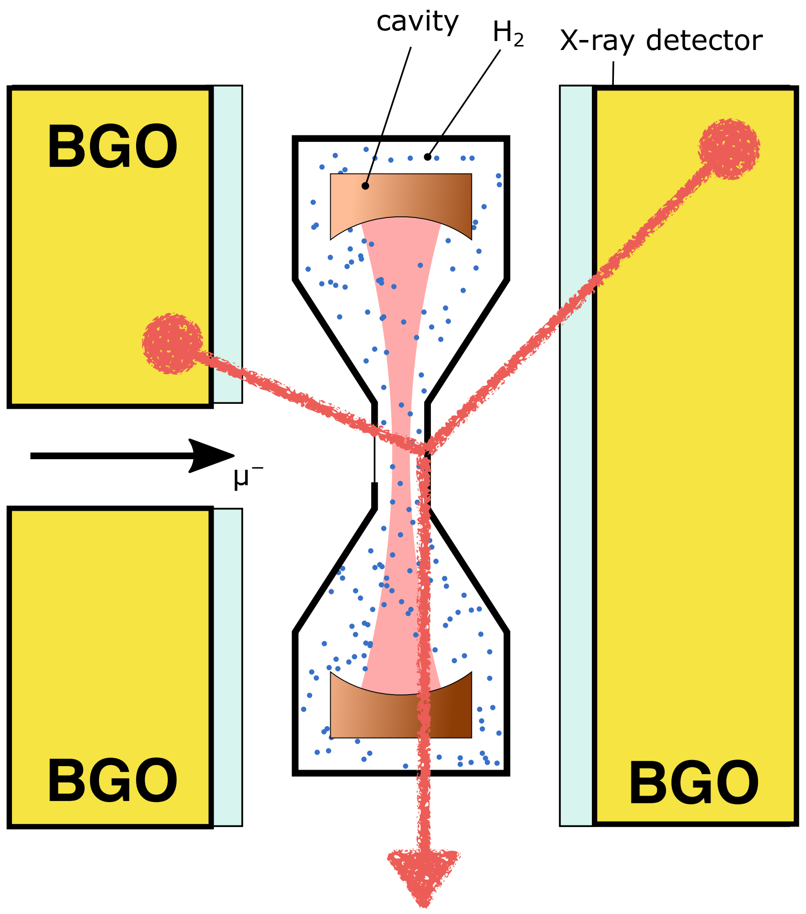

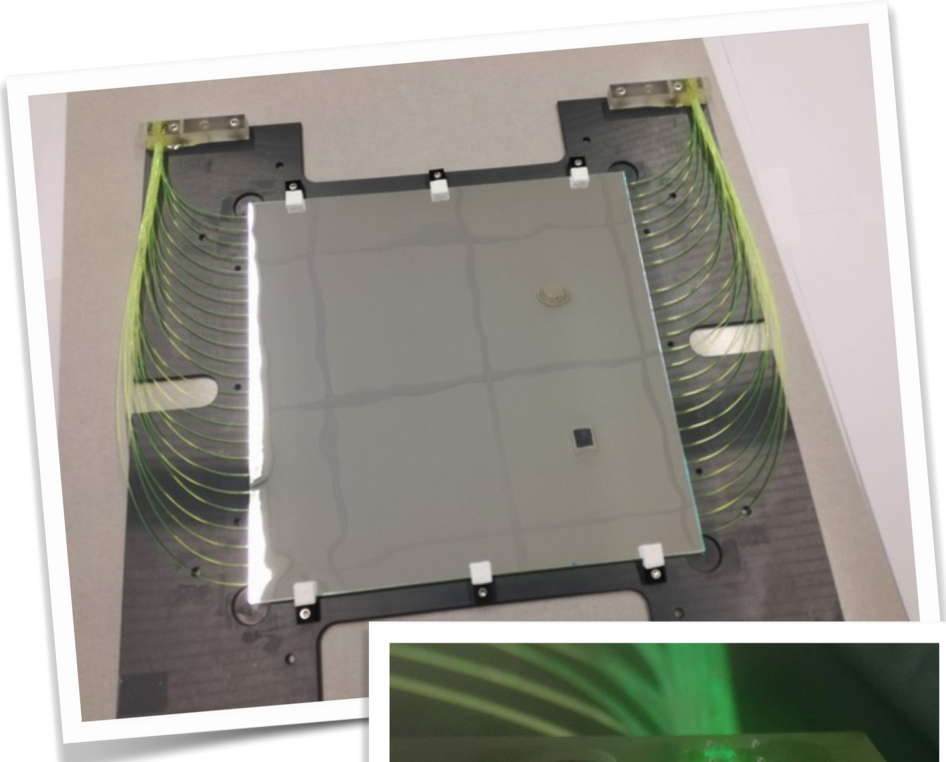

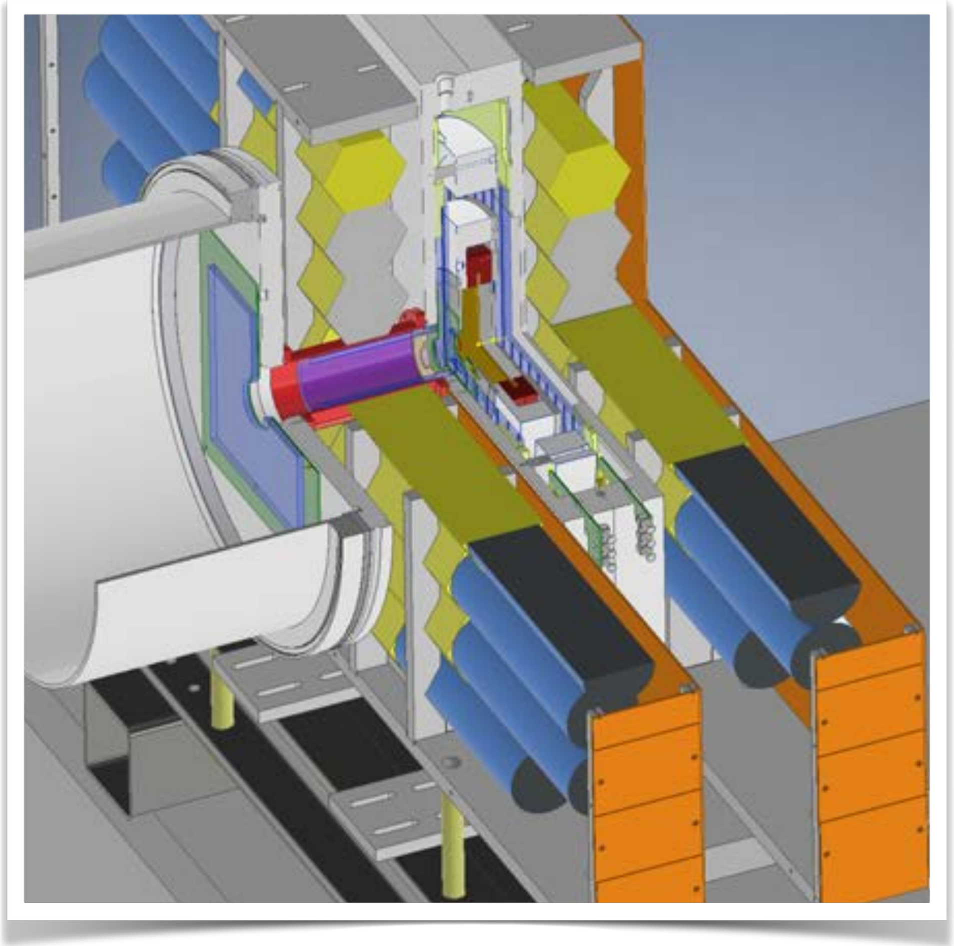

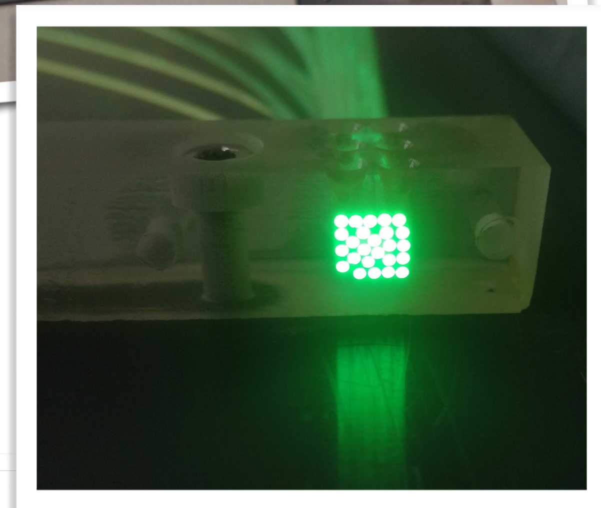

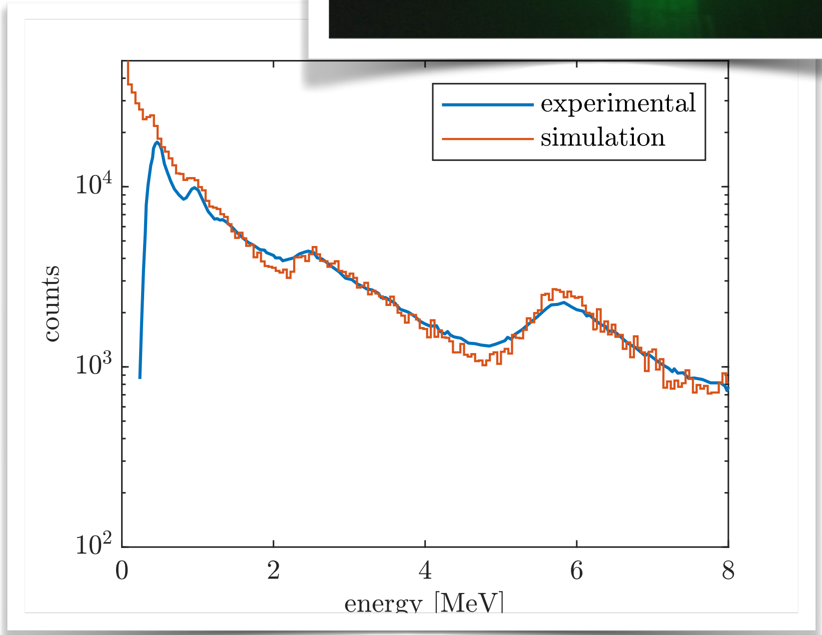

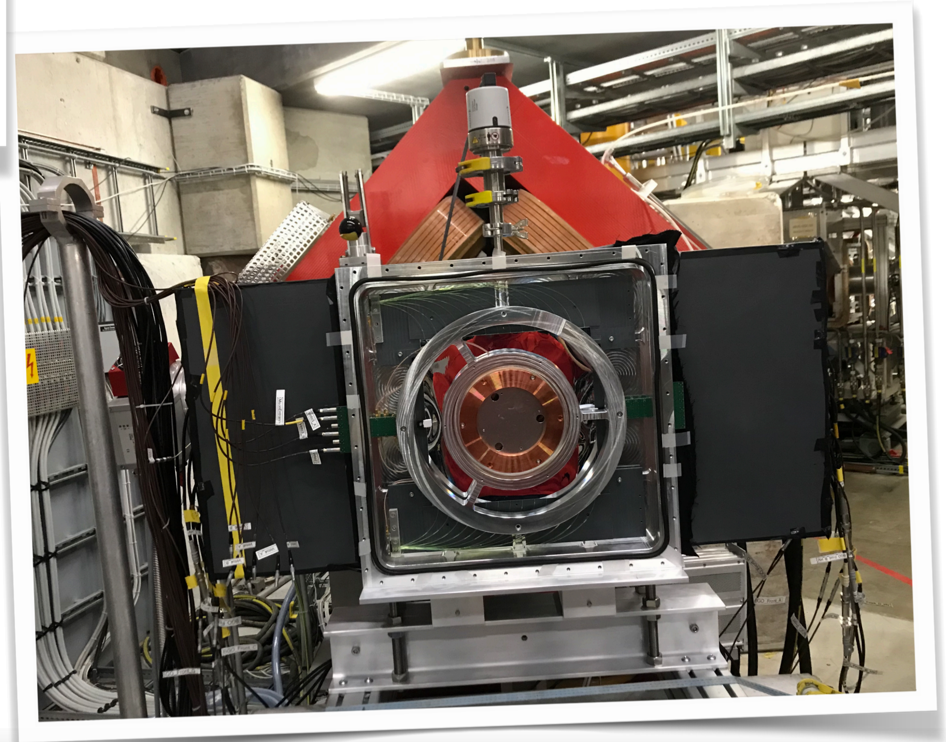

- Realised a system with two BGO clusters for efficient detection of MeV X-Rays
- Several large size plastic scintillators for rejection of decay-electrons

L. Sinkunaite, PhD Thesis, ETH 2021

Results from the detection system

- ☑ Detection efficient for μAu events: 80%
- ☑ False identification of muon-decay events: 10%
- ☑ Anti-coincidece efficiency: >95%
- ☑ Uncorreletaed background quantified

Estimated background and event rates

$$\begin{aligned} P_{\text{signal}} &= 400 \text{ events/h} \\ P^{\text{BG}}_{\text{diffusion}} &= 2500 \text{ events/h} \\ P^{\text{BG}}_{\text{electron}} &= 800 \text{ events/h} \\ P^{\text{BG}}_{\text{uncorrelated}} &= 500 \text{ events/h} \end{aligned}$$

These numbers depends on various still unknown factors as laser and cavity performance, muon beam etc

The laser system

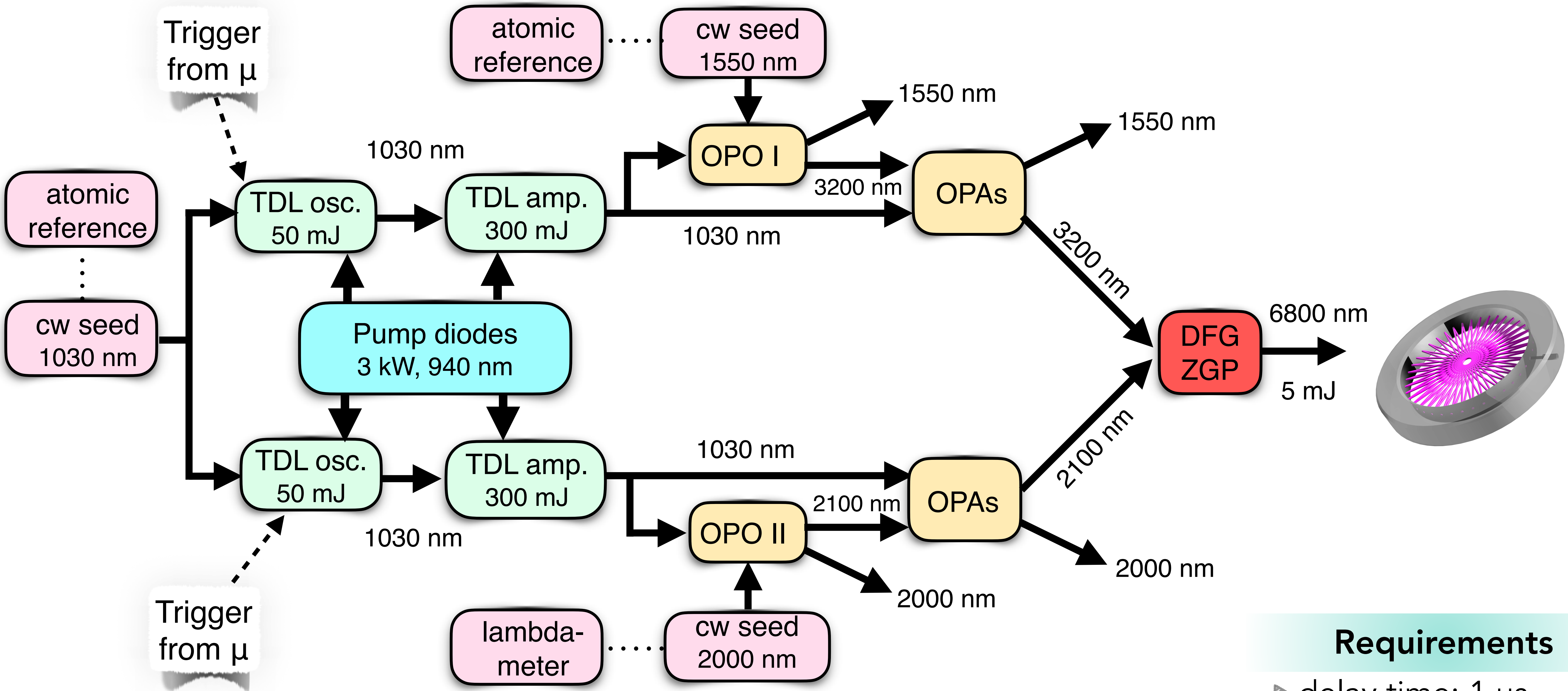

Requirements

- delay time: 1 µs
- stochastic trigger
- energy: 5 mJ
- repetition rate: 200 1/s
- wavelength: 6.8 µm
- bandwidth: < 100 MHz

Single-frequency thin-disk laser oscillator

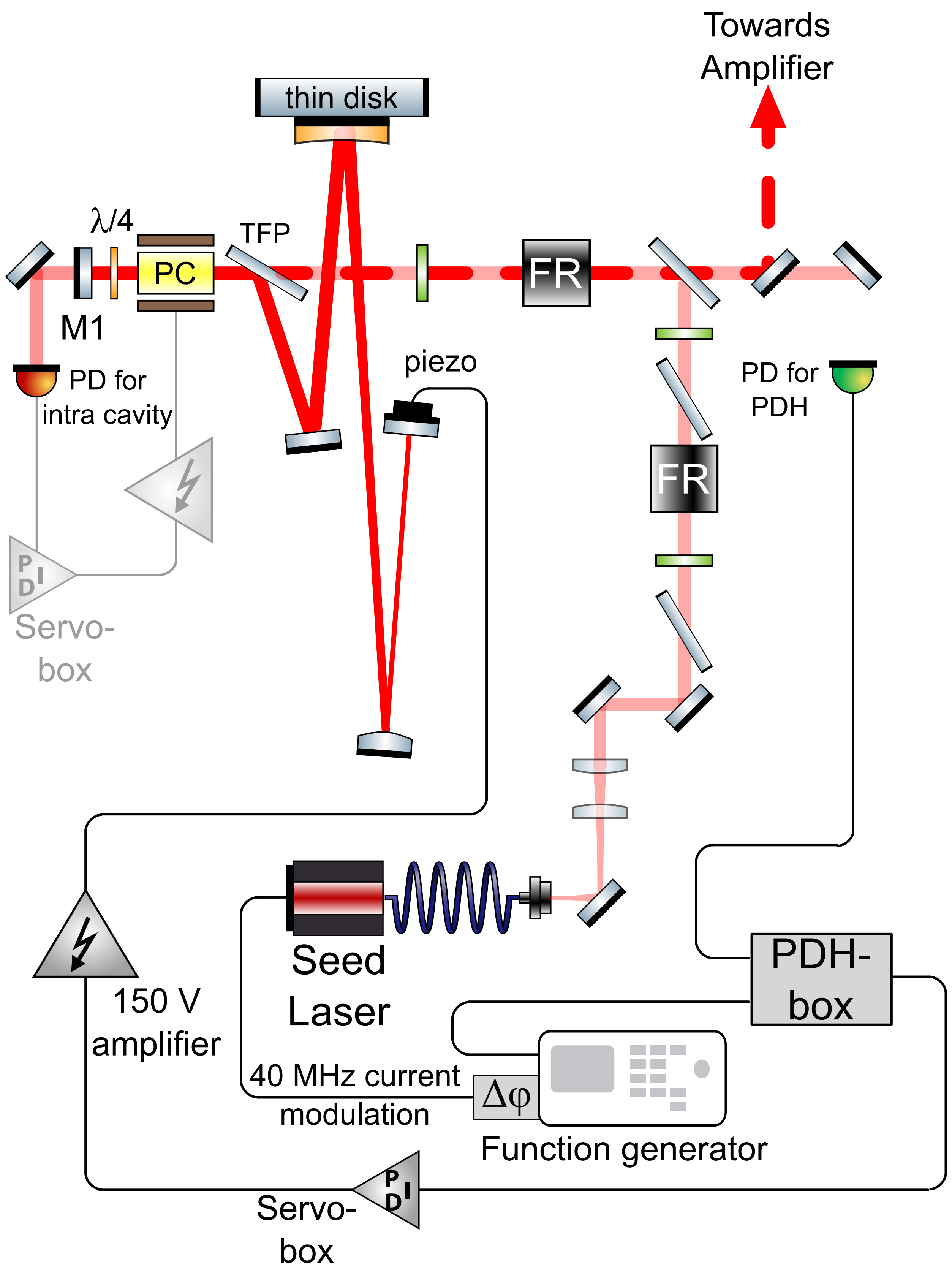

M. Zeyen , PhD Thesis, ETH 2021

- ☐ Energy: 32 mJ
- ☑ Delay: 700 ns
- ☑ Pulse-to-pulse stability: 1% (rms)
- ☑ Single-frequency operation
- ☑ Laser chirp < 2 MHz
- ☑ Continuos re-locking

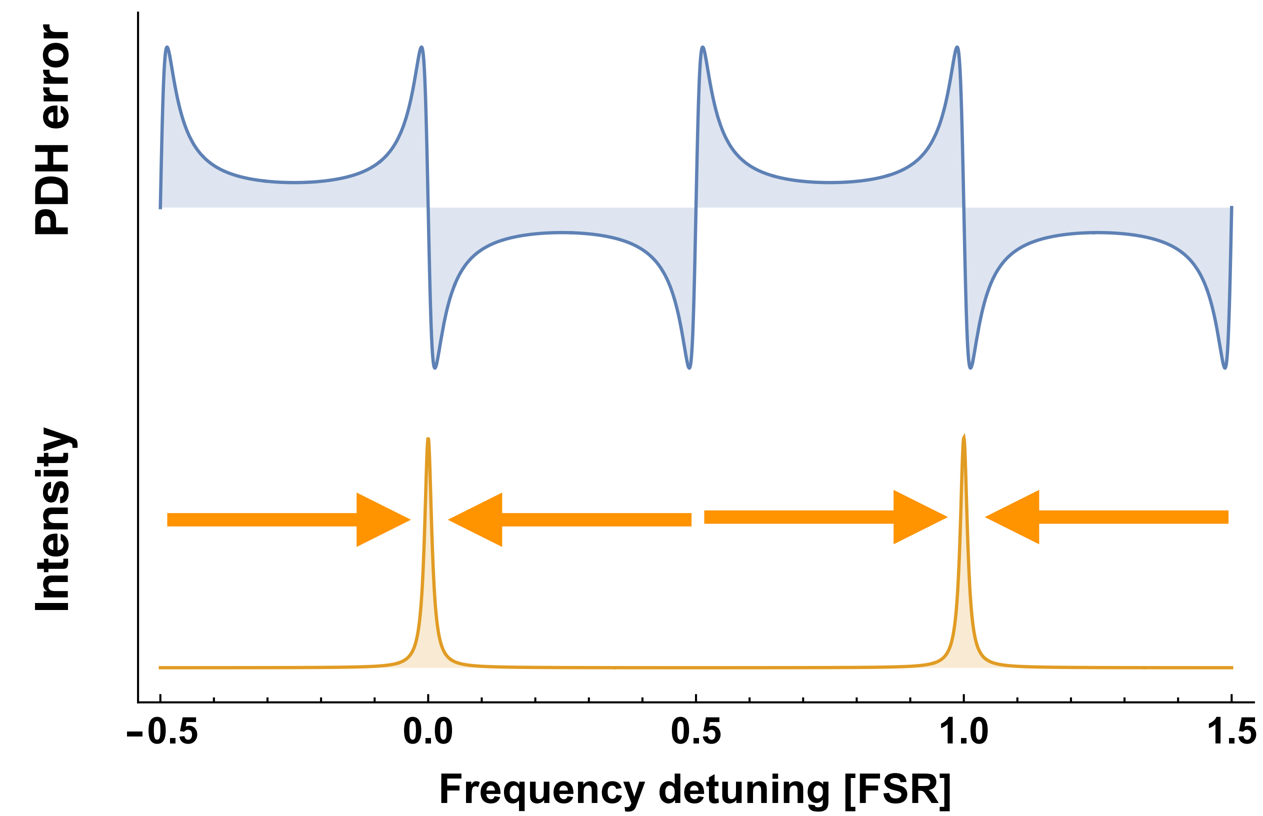

Thin-disk laser amplifier

The sequence

4f
amplification
Fourier Transform
amplification
4f
4f
amplification
Fourier Transform
amplification
4f
4f
amplification
Fourier Transform
amplification
4f
4f

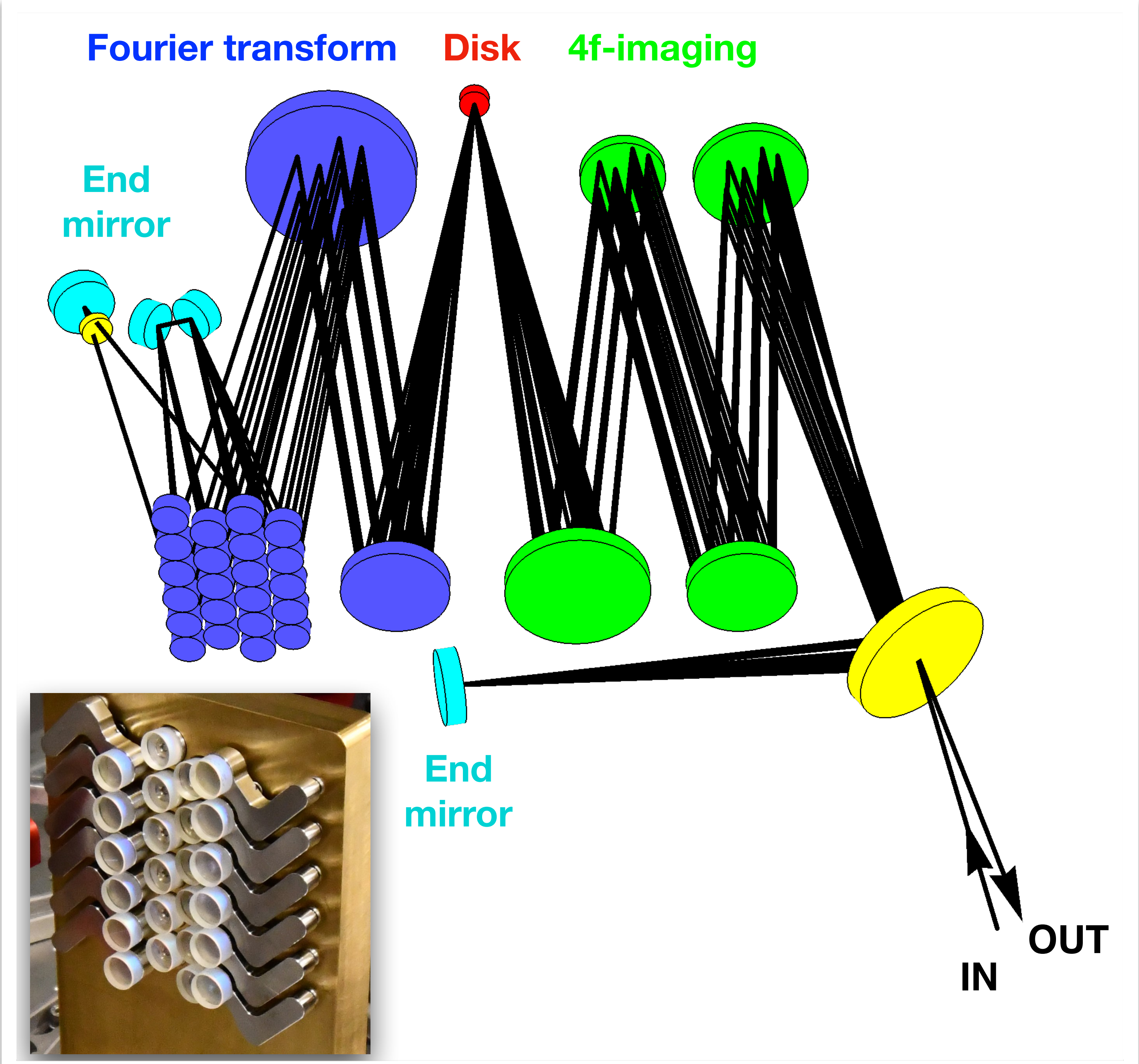

- [x] Energy: 220 mJ
- [x] Gain: 7.5
- [x] Beam quality: M^2=1.05
- [x] Pointing stability
- [x] Insensitive to thermal lens

- [ ] Increase beam size
- [ ] Astigmatism compensation
- [ ] New disks
- [ ] Energy: 300 mJ

M. Zeyen, PhD Thesis, ETH 2021

The laser system

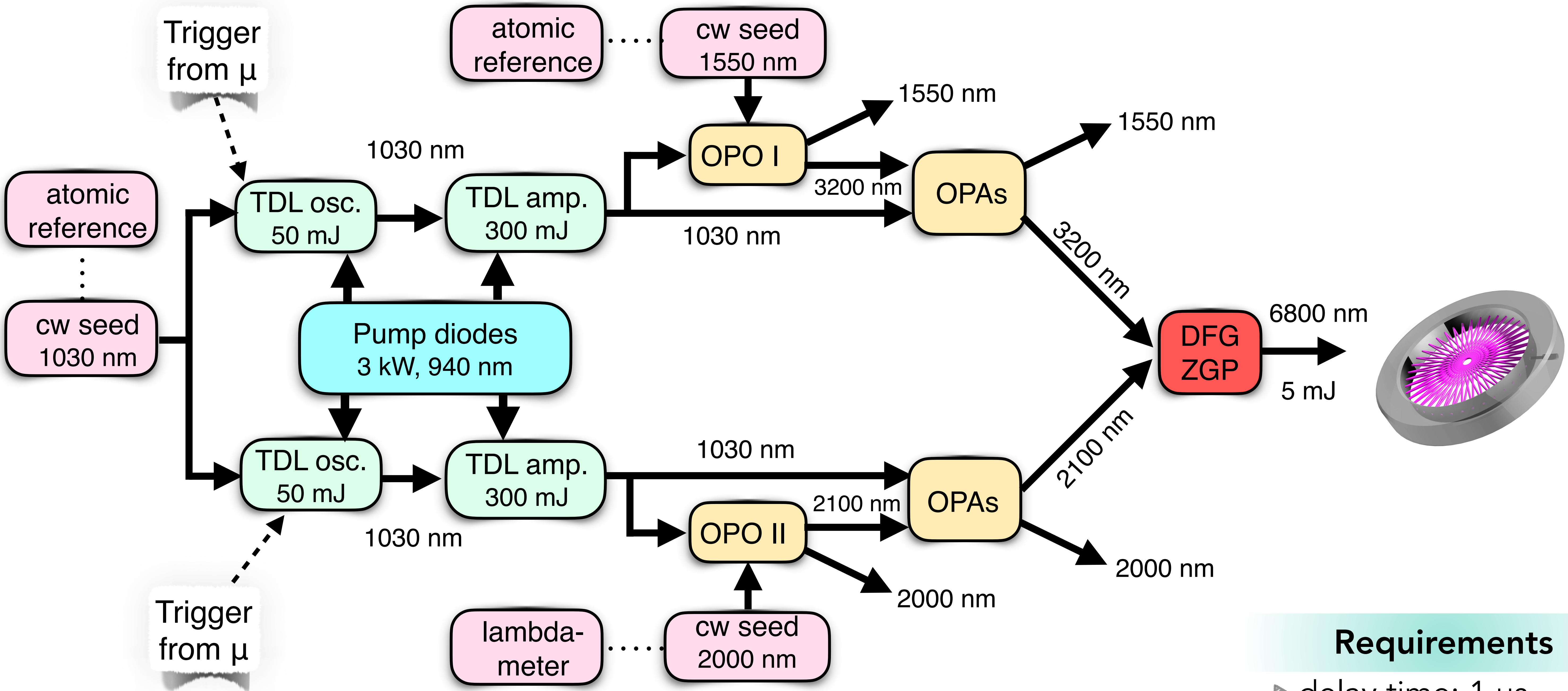

Requirements

- delay time: 1 µs
- stochastic trigger
- energy: 5 mJ
- repetition rate: 200 1/s
- wavelength: 6.8 µm
- bandwidth: < 100 MHz

Sketch of the down-conversion stages (in preparation)

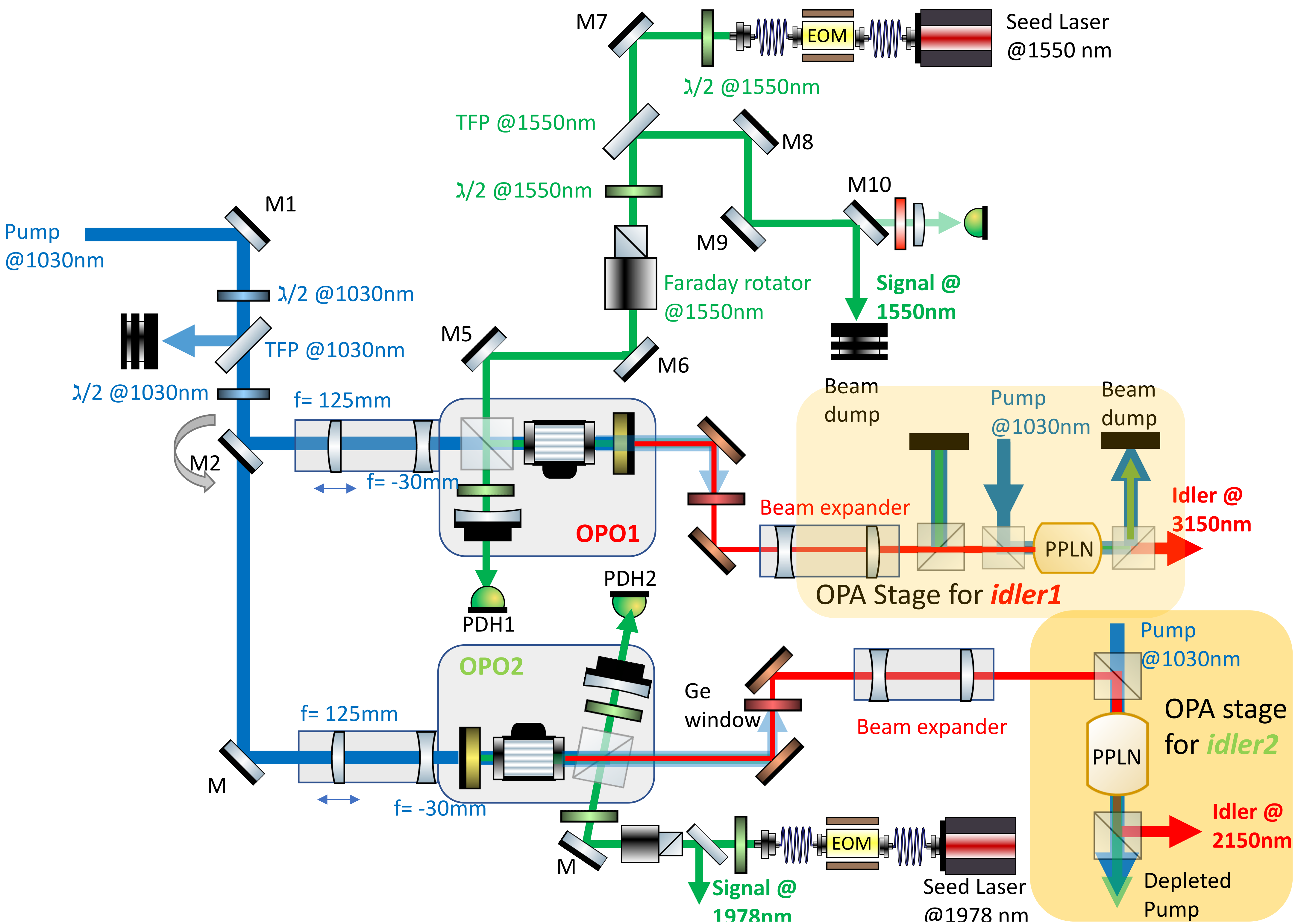

- Cavity with tunable Q-factor
- Injection seeded OPOs

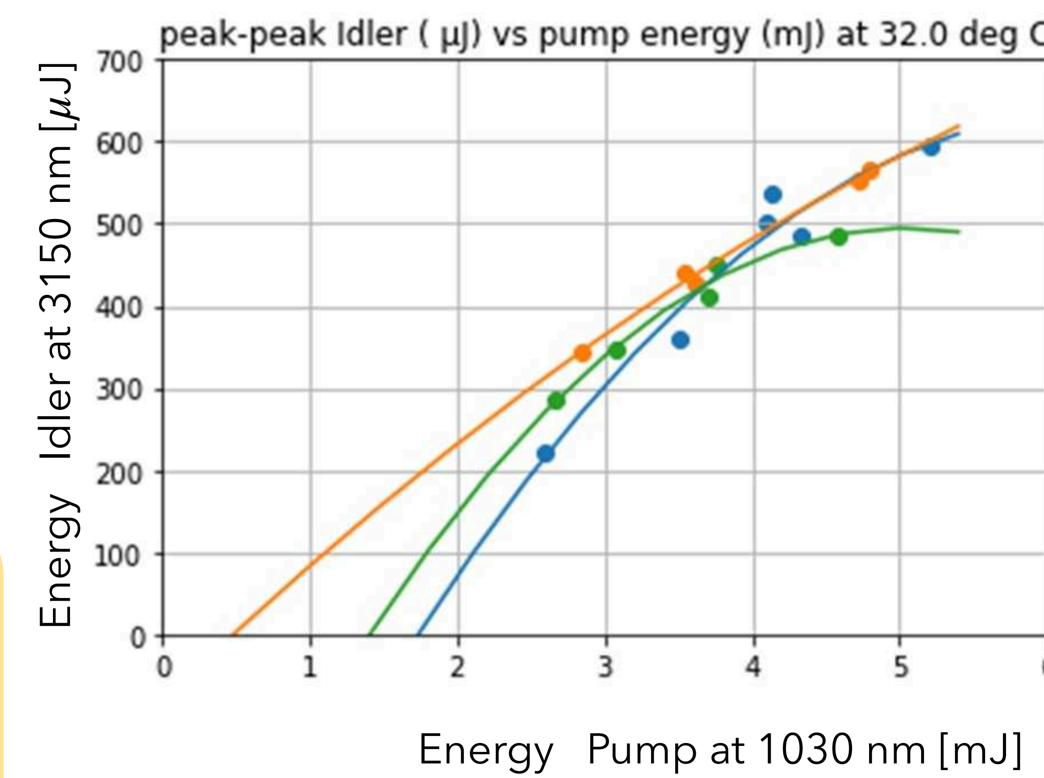

The multi-pass cavity

The two cavity types under development

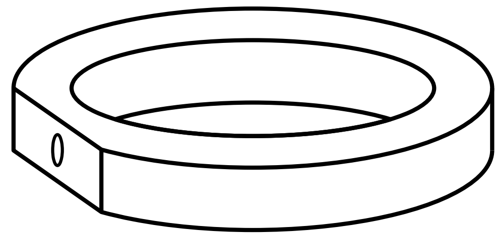

- Resonant vertically
- Unstable horizontally

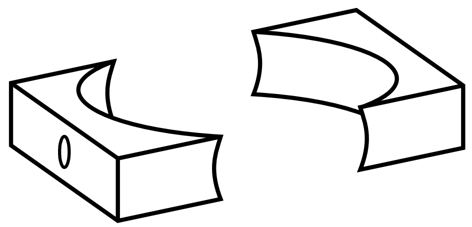

- Resonant vertically
- Stable horizontally

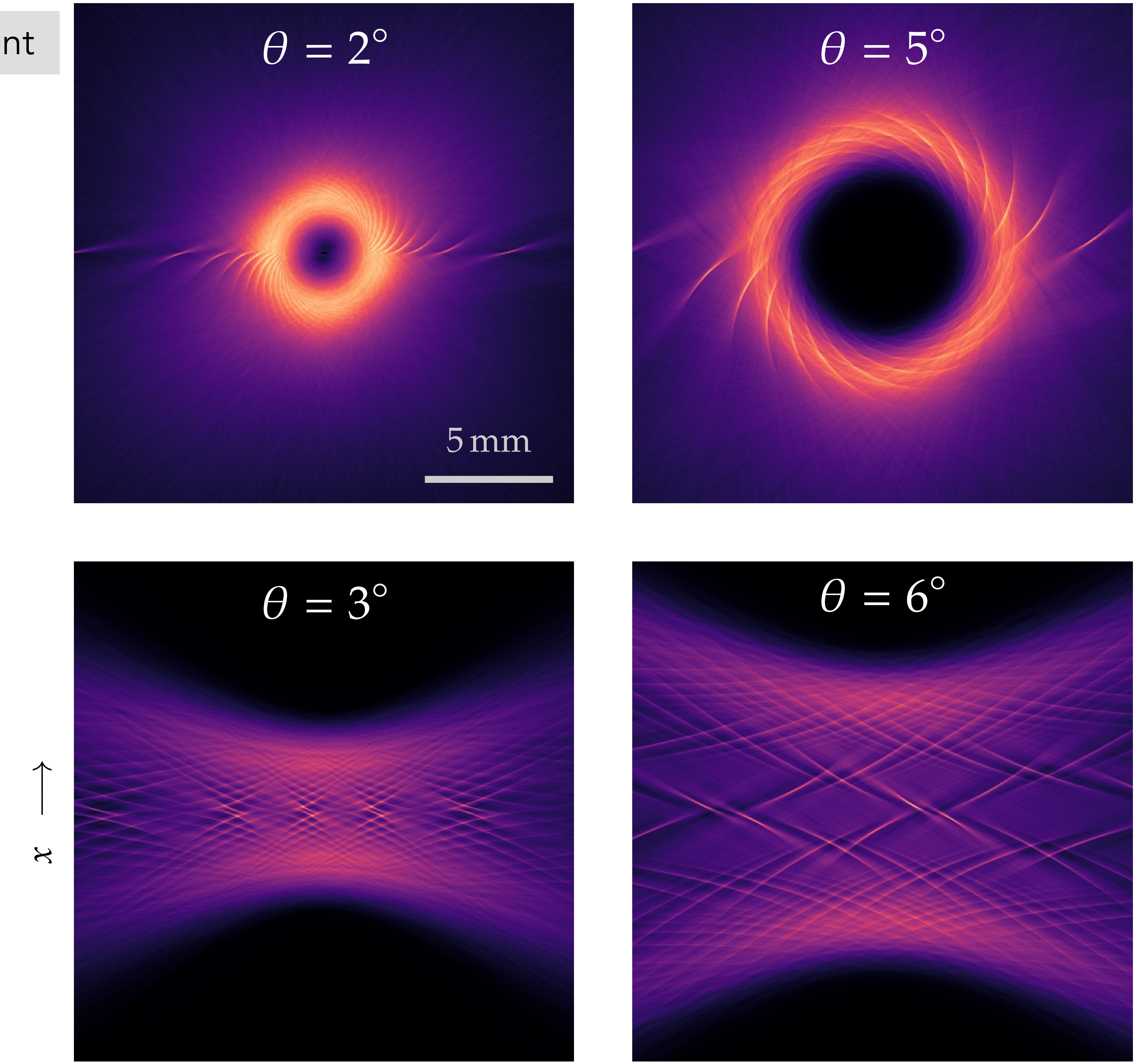

M. Marszalek, PhD Thesis, ETH 2022

Simulated laser fluence

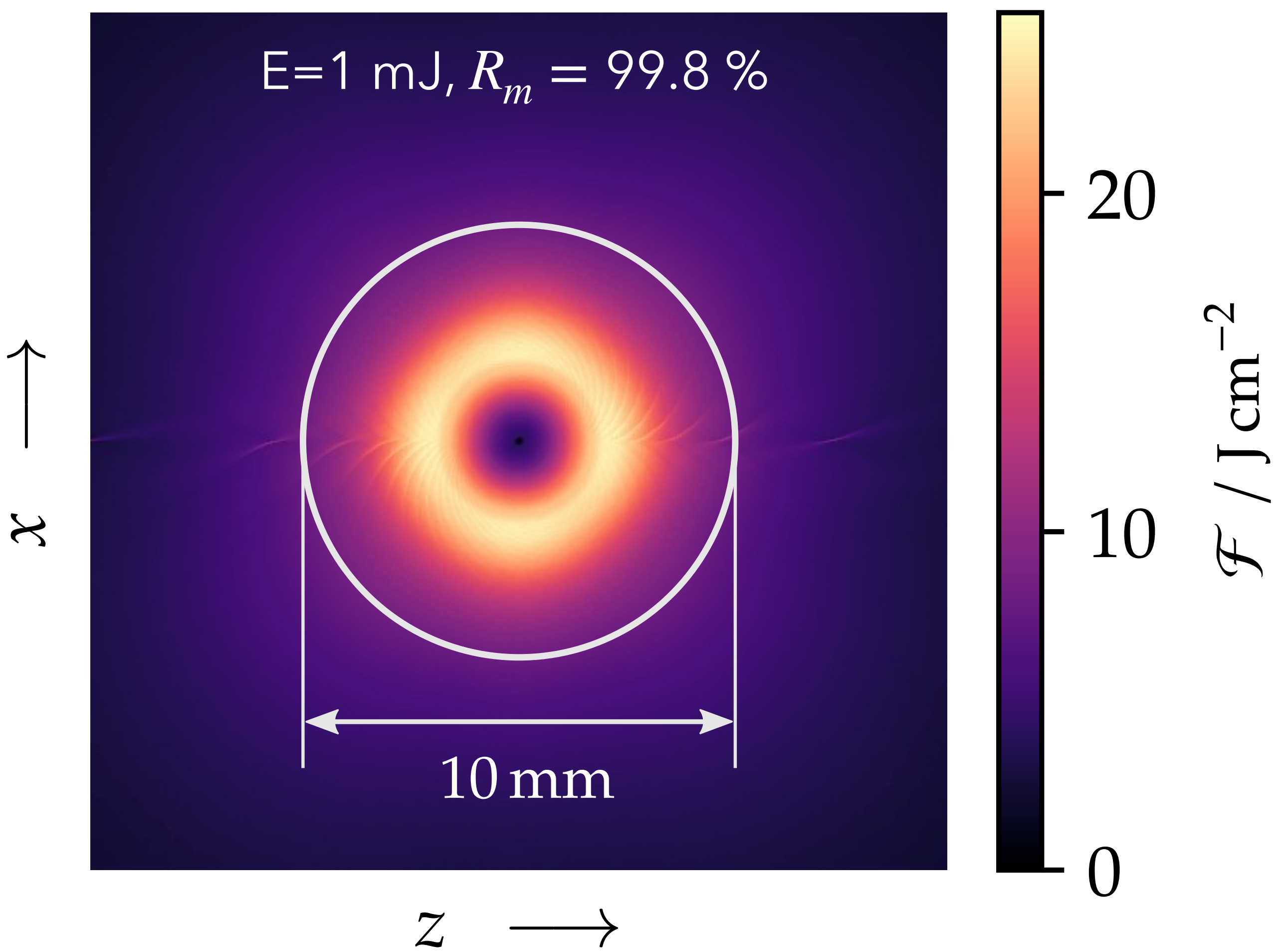

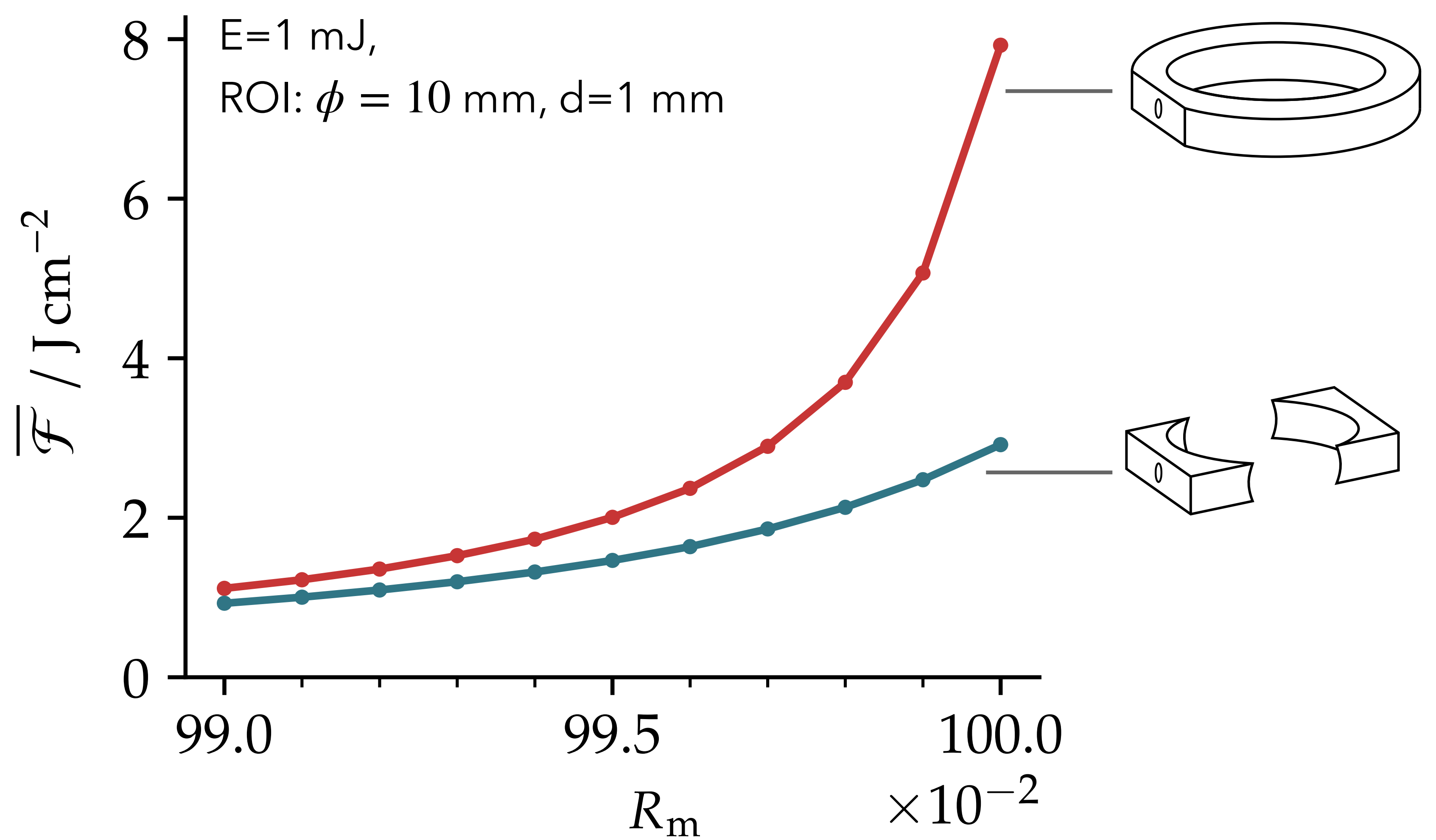

M. Marszalek , PhD Thesis, ETH 2022

The various passes in the toroidal cavity

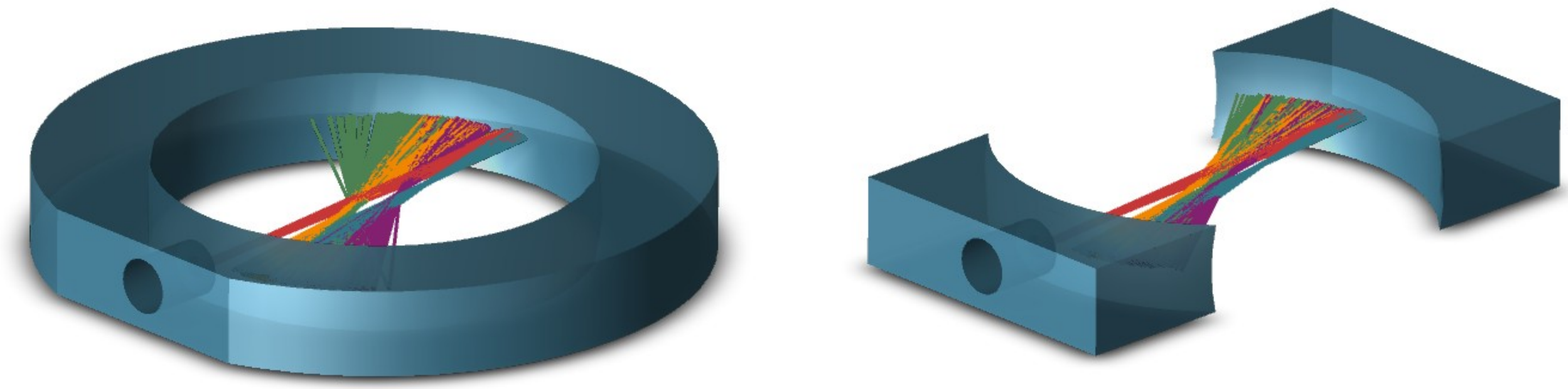

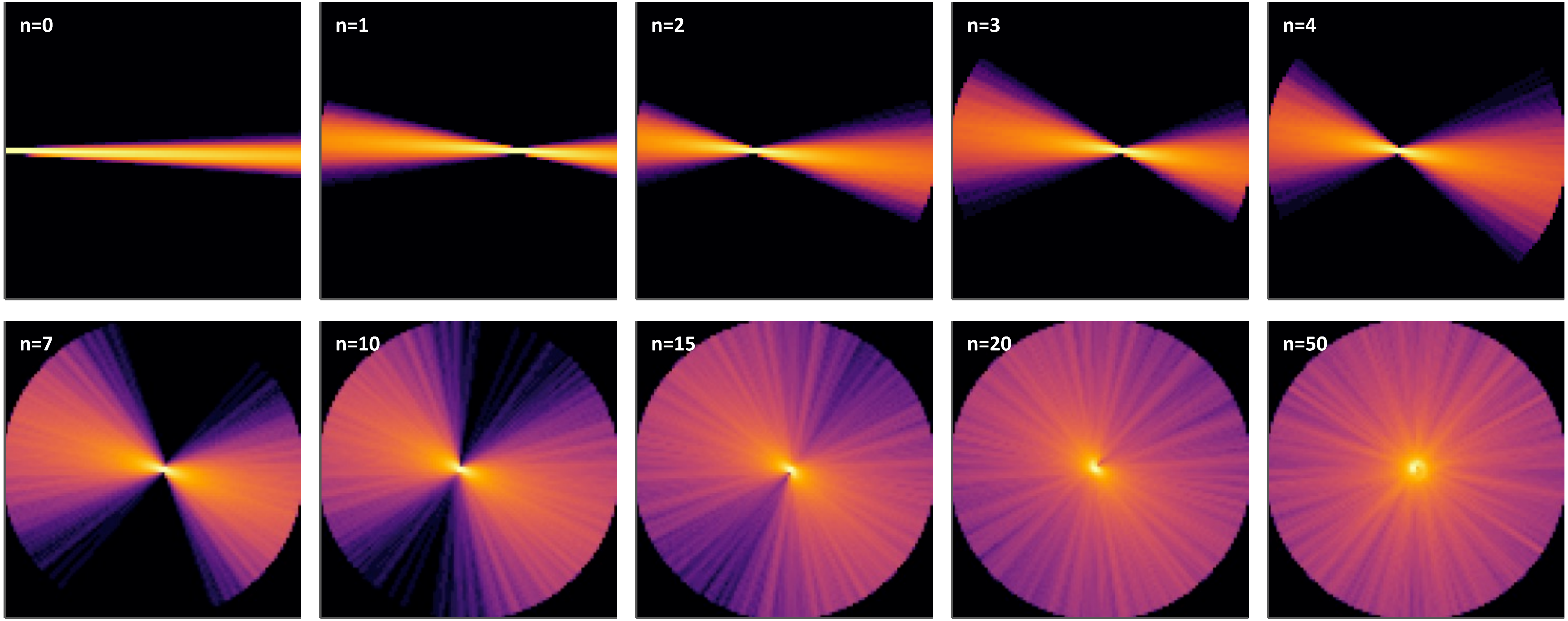

Qualify cavity with ring-down techniques

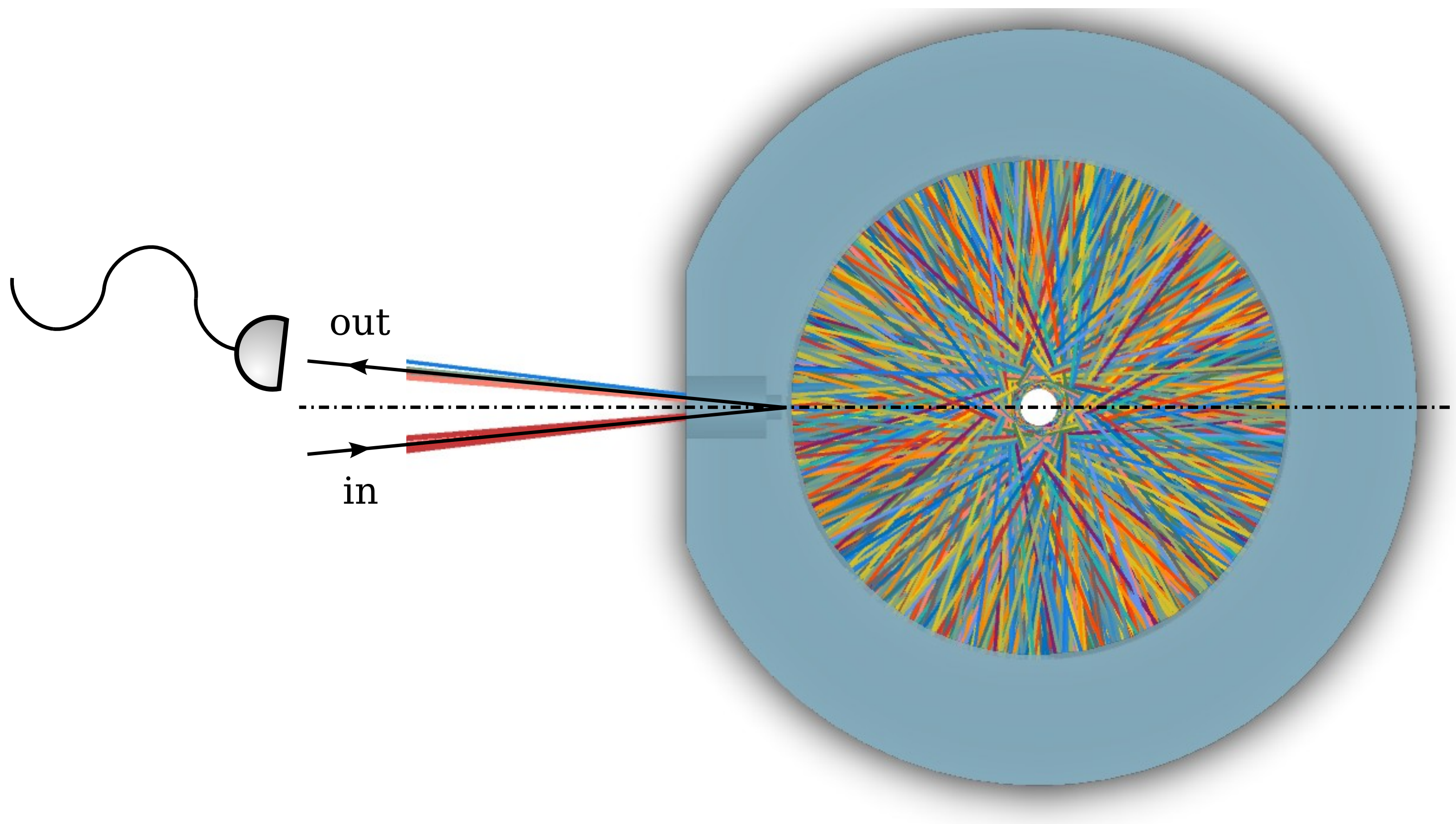

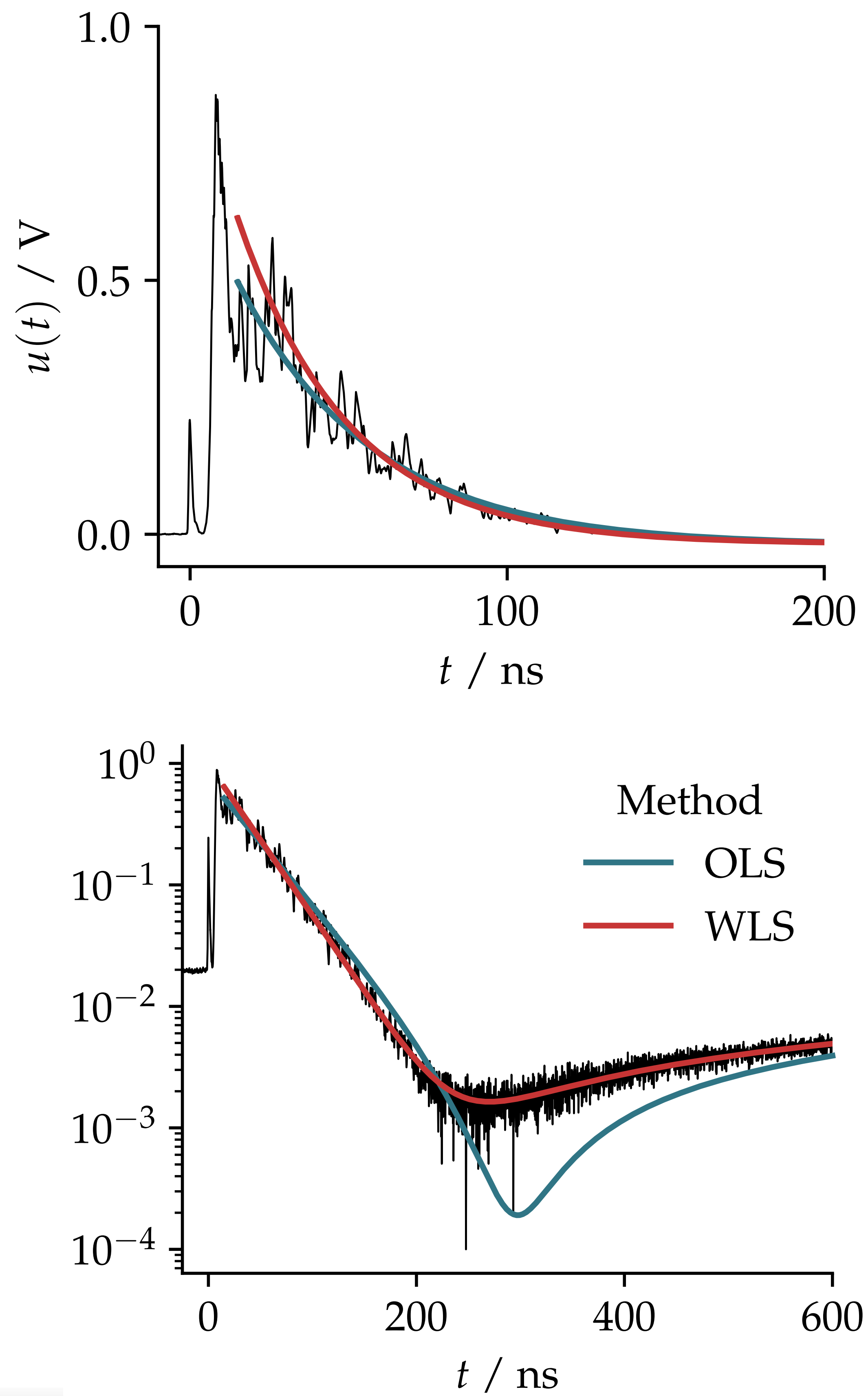

- Use ps laser pulses
- Measure light escaping through the input slit
- Developed a model for the variance und used to fit the data

Results for the two measured cavities

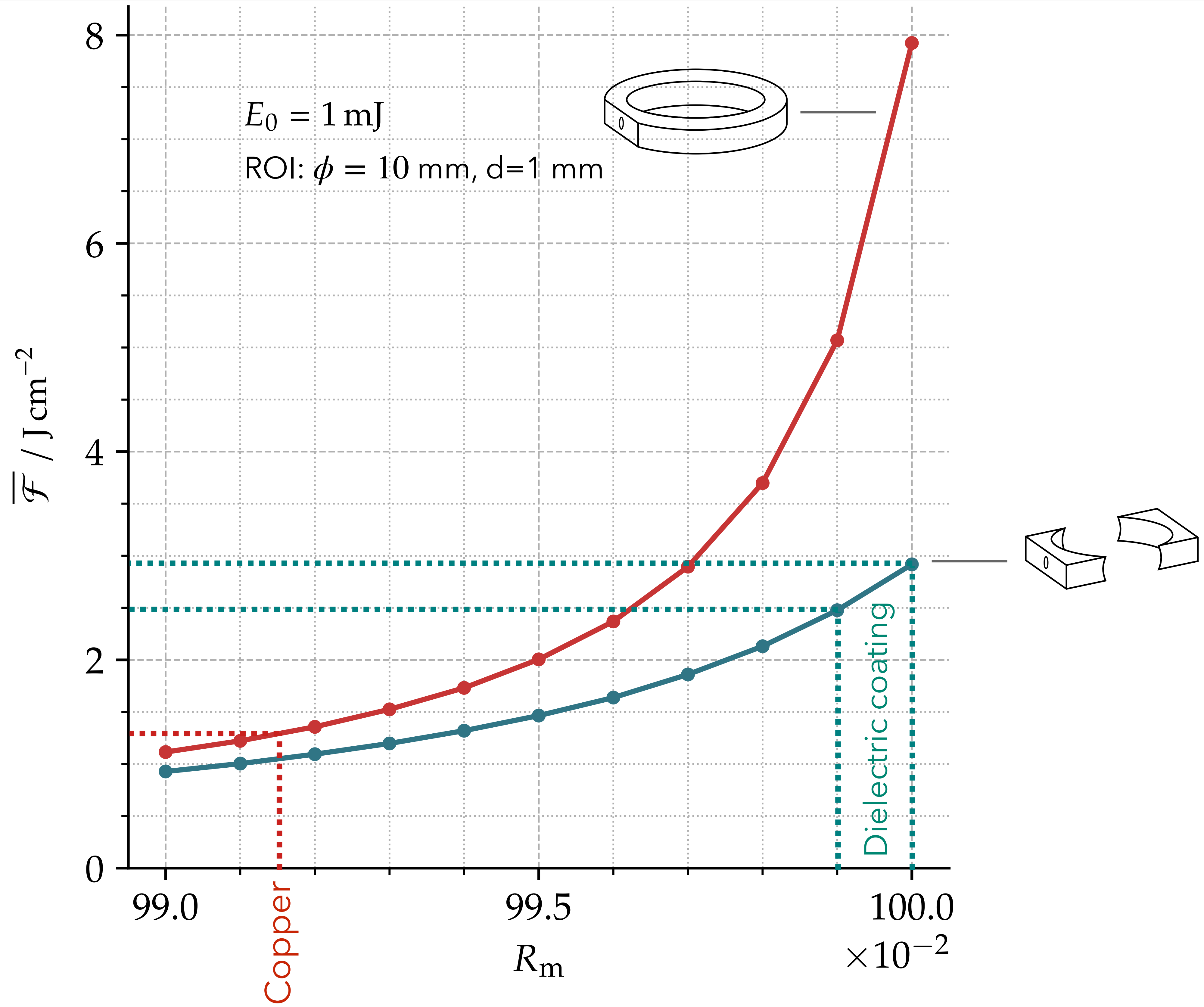

- ☑ Developed two cavity designs
- ☑ Cavities perform as expected
- ☑ Developed monitoring method

- ☐ Development of a dielectric coating for the toroidal cavity
- ☐ Losses in 1 mm slit?
- ☐ Alignment of two-mirror cavity not trivial
- ☐ Test at cryogenic temperatures

Transition probabilities ρ_{33} in ROI for 1 mJ

Copper, toroidal: 3%

Dielectric, two-mirror: 6%

Summary of status

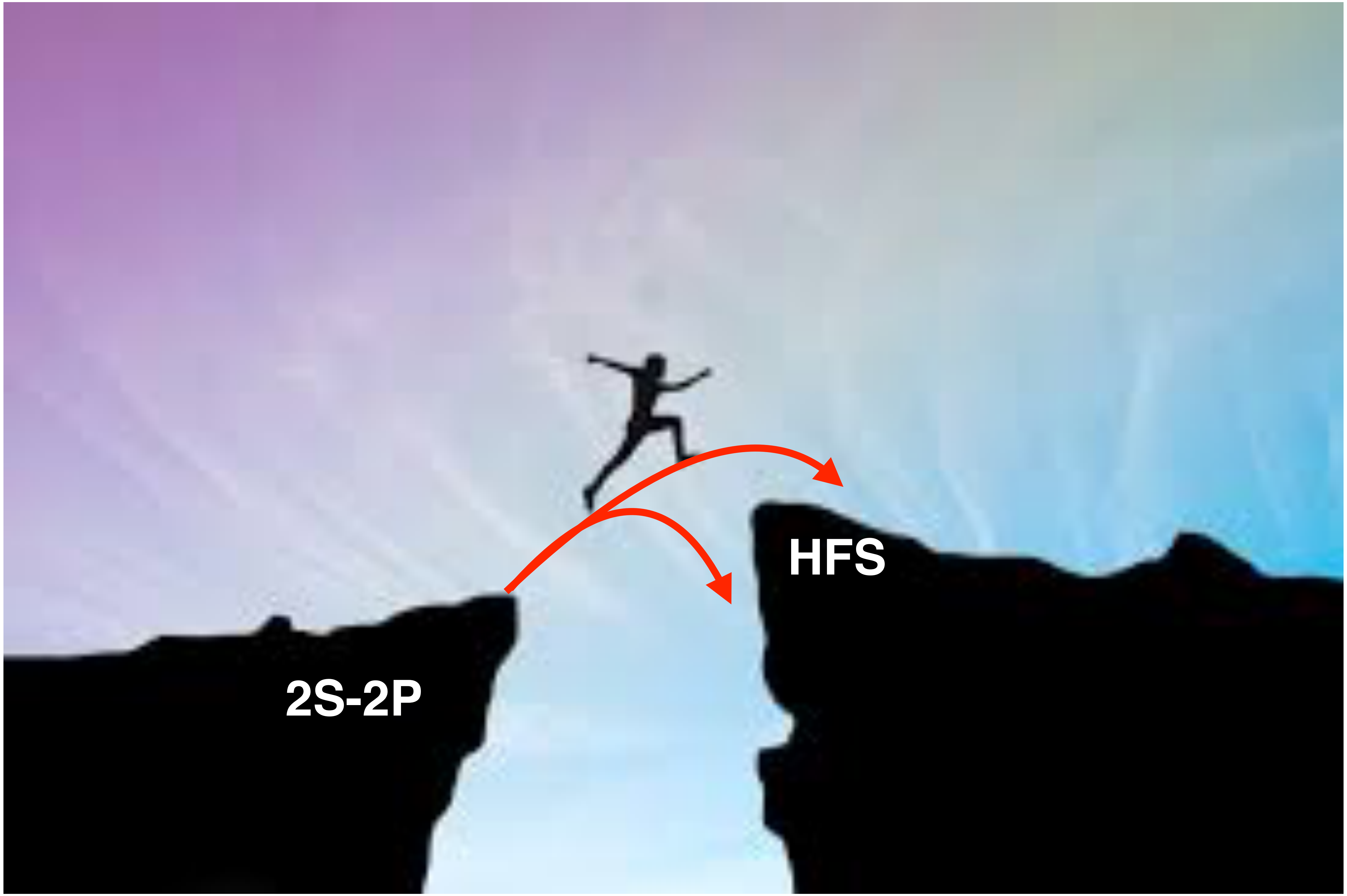

Message to theorists

There is a need to improve on the HFS theory of μp and H.

- ☑ This will simplify tremendously the experimental efforts
- ☑ This will pay off after the measurement of the muonic HFS resonance
- ☑ Combining H with μp will result in testing QED for a hyperfine splitting on the ppt level

Present theory uncertainty:

- ☐ 7 μeV from QED in μp (very conservative estimate)
- ☐ 2 μeV from 2γ-contribution (limited by recoil-finite-size contribution)

If you have new fits of G_E, G_M, F_1, F_2

–> gratis publication of the recoil contribution for H and μp

$$\Delta_{\rm recoil} = \frac{Z\alpha}{\pi(1+\kappa)}\int_0^\infty \frac{\mathrm{d}Q}{Q}\left\{\frac{8mM}{v_l+v}\frac{G_M(Q^2)}{Q^2}\left(2F_1(Q^2)+\frac{F_1(Q^2)+3F_2(Q^2)}{(v_l+1)(v+1)}\right) - \frac{8m_r\,G_M(Q^2)G_E(Q^2)}{Q} - \frac{m}{M}\frac{5+4v_l}{(1+v_l)^2}F_2^2(Q^2)\right\}.$$

The CREMA collaboration

Laboratoire Kastler Brossel
Physique quantique et applications

F. Biraben, P. Indelicato, L. Julien, F. Nez, N. Paul, P. Yzombard

MAX-PLANCK-INSTITUT FÜR QUANTENOPTIK GARCHING

T.W. Hänsch

JOHANNES GUTENBERG UNIVERSITÄT MAINZ

Ouf, R. Pohl, S. Rajamohanan, F. Wauters

國立清華大學
NATIONAL TSING HUA UNIVERSITY

Y.-H. Chang, W.-L. Chen, Y.-W. Liu, L.-B. Wang

PAUL SCHERRER INSTITUT PSI

ETH

L. Affoltern, D. Göldi, O. Kara, K. Kirch, F. Kottmann, J. Nuber, K. Schuhmann, D. Taqqu, M. Zeyen, A. Antognini, M. Hildebrandt, A. Knecht, M. Marszalek, L. Sinkunaite, A. Soter

UNIVERSIDADE NOVA DE LISBOA

P. Amaro, P.M. Carvalho, M. Ferro, M. Guerra, J. Machado, J. P. Santos, L. Sustelo

UNIVERSIDADE DE COIMBRA

F.D. Amaro, L.M.P. Fernandes, C. Henriques, R.D.P Mano, C.M.B. Monteiro, J.M.F. dos Santos, P. Silva

IFJ PAN

A. Adamczak

IFSW
UNIVERSITÄT STUTTGART
INSTITUT FÜR STRAHLWERKZEUGE
STUTTGART LASER TECHNOLOGIES

M. Abdou-Ahmed, T. Graf